Human mobility amid emerging sedentism in the central Zagros: laser ablation strontium isotope analysis at early Neolithic Bestansur, Iraqi Kurdistan

frontiers in Environmental Archaeology

TYPE Original Research
PUBLISHED 23 April 2026
DOI 10.3389/fearc.2026.1818214

OPEN ACCESS

EDITED BY
Michelle S. Eusebio,
University of the Philippines Diliman, Philippines

REVIEWED BY
George Kamenov,
University of Florida, United States
Berta Morell,
University of Barcelona, Spain

*CORRESPONDENCE
Giulia Ragazzon
g.ragazzon@pgr.reading.ac.uk

RECEIVED 26 February 2026
REVISED 26 March 2026
ACCEPTED 30 March 2026
PUBLISHED 23 April 2026

CITATION
Ragazzon G, Matthews R, Milton JA, van Acken D, Raeuf Aziz K and Pryor AJE (2026) Human mobility amid emerging sedentism in the Central Zagros: laser ablation strontium isotope analysis at Early Neolithic Bestansur, Iraqi Kurdistan. *Front. Environ. Archaeol.* 5:1818214. doi: 10.3389/fearc.2026.1818214

Human mobility amid emerging sedentism in the Central Zagros: laser ablation strontium isotope analysis at Early Neolithic Bestansur, Iraqi Kurdistan

Giulia Ragazzon[1,2]*, Roger Matthews[1], James A. Milton[3], David van Acken[4], Kamal Raeuf Aziz[5] and Alexander J. E. Pryor[2]

[1]Department of Archaeology, University of Reading, Reading, United Kingdom, [2]Department of Archaeology and History, University of Exeter, Exeter, United Kingdom, [3]School of Ocean and Earth Sciences, University of Southampton, Southampton, United Kingdom, [4]UCD School of Earth Sciences, University College Dublin, Dublin, Ireland, [5]Slemani Directorate of Antiquities and Heritage, Kurdistan Regional Government, Sulaymaniyah, Iraq

The Neolithic of Southwest Asia (c. 10,000–5,200 BCE) is associated with increasing residential stability alongside resource domestication processes. Yet, the trajectories of sedentism varied widely, with balances between sedentary and mobile behaviors contextually driven by subsistence needs, cultural practices and expanding interaction networks. In the Central Zagros, a key area for early domestication and settled life, the role of human mobility in shaping resource procurement and community structure remains underexplored. To investigate this, high-resolution laser ablation strontium isotope analysis was applied to 101 human teeth (41 individuals) from Bestansur (Iraqi Kurdistan), a major 8th-millennium BCE center in the region, using a life-course approach. The results, supported by new, multi-proxy baseline data, delineate a largely local community with multi-generational ties to the site, while providing possible evidence for the exploitation of different foraging locales. Challenging rigid dichotomies between mobile hunter-gatherers and settled farmers, the integration of isotopic and contextual data enables consideration of diverse landscape use amid emerging sedentism, offering direct insights into Early Neolithic community make-up. Additionally, it contributes to the characterization of strontium isotope variability in a region with sparse isotope records, providing grounds for discussions of mobility and landscape use that transcend specific chronological boundaries.

KEYWORDS
Central Zagros, human mobility, laser ablation, neolithic, strontium isotope analysis

1 Introduction

The development of sedentary lifeways during the Neolithic (c. 10,000–5,200 BCE) profoundly transformed human-environment relationships in Southwest Asia. This process, linked but not always synchronous with the emergence of domestication and agriculture (Dow and Reed, 2015; Zeder, 2024a), saw highly mobile groups progressively commit to select locales, forming settled communities. Yet, its pace and trajectories, along with food procurement and cultural changes, varied across regions. In particular, the balance between sedentary and mobile behaviors is likely to have been contextually dynamic, driven by needs, choices, and factors such as climate and resource availability (Gregoricka, 2021). Over the last 15 years, the role of human mobility in shaping and sustaining settled communities has been increasingly explored through direct analyses of human remains (e.g. Alt et al., 2013; Santana et al., 2021; Knipper et al., 2023; Pearson et al., 2023; Wang et al., 2023a,b; Plug et al., 2025). However, research has primarily focused on Anatolia and the Levant, leaving the eastern part of the Fertile Crescent comparatively understudied.

The Central Zagros, encompassing the uplands and lowlands of Eastern Iraq and Western Iran, have long been recognized as a theater for independent experiments with domestication and sedentism (Matthews et al., 2020a; Daly et al., 2021; Darabi, 2022; Zeder, 2024a). Additionally, autonomous population development has been highlighted by ancient DNA studies, which have identified Early Holocene individuals from the region as the most genetically distinct in Southwest Asia (Broushaki et al., 2016; Lazaridis et al., 2016; Altınışık et al., 2022). Archaeological, zooarchaeological and archaeobotanical evidence suggests that a major transition from seasonal site occupation to permanent, year-round settlements took place in the Central Zagros between 8,500 and 7,000 BCE (Zeder, 2024a). Despite a general increase in residential stability, it has been proposed that logistical movements for resource acquisition retained their importance long after the adoption of sedentary lifeways, influenced by the slow adaptation of food procurement and cultural practices (Zeder, 2024a), and by the expansion of exchange networks (Watkins, 2023). However, aside from two studies reporting human mobility data for the lowland site of Ali Kosh, in the Iranian Zagros (Darabi et al., 2024; Ávila et al., 2026) and Nemrik, in northern Iraq (Ávila et al., 2026), the lack of systematic research into mobility dynamics in the Eastern Fertile Crescent has limited an in-depth understanding of human movement and its contribution to community make-up during this formative period. The availability of a large osteological assemblage from Bestansur, a major 8th-millennium BCE site in the Iraqi Zagros, offers an opportunity to address this gap using a human-centered approach.

Continued advancements in strontium isotope analysis ($^{87}Sr/^{86}Sr$), a well-established tool for the study of mobility (Bentley, 2006; Britton, 2020), have considerably enhanced fine-scale reconstructions of past human movement. Laser ablation multi-collector inductively coupled plasma mass spectrometry (LA-MC-ICP-MS) now enables the rapid acquisition of $^{87}Sr/^{86}Sr$ profiles measured at high spatial resolution across sequentially formed dental enamel (Pryor et al., 2020; Linscott et al., 2023). Here, we applied this technique to 101 teeth belonging to 41 individuals from Bestansur, with the aim of investigating life-course mobility and its intersections with sociocultural structures at the transition to sedentism. Human $^{87}Sr/^{86}Sr$ profiles are contextualized using a multi-proxy baseline constructed for the site. In addition, we report baseline data for four other archaeological sites in the Central Zagros (two in Iraq and two in Iran; Figure 1, Supplementary Text S1 and Figures S1–S4, S7), contributing to the characterization of $^{87}Sr/^{86}Sr$ variability in a region with sparse isotope records.

1.1 Archaeological context

Located in the Sulayimaniyah province of Iraqi Kurdistan, the site of Bestansur (35 °22'36.7 *N*, 45 °38'44.4 E; c. 550 m asl) occupies a low natural rise with access to a perennial karst spring in the Sharizor plain, on the western foothills of the Central Zagros (Figures 2a, b). Since 2012, it has been investigated by the University of Reading and the Slemani Directorate of Antiquities and Heritage as part of the Central Zagros Archaeological Project (CZAP), marking the resumption of Neolithic research in the region after a long archaeological hiatus (Matthews et al., 2020a; Zeder, 2024a,b). Absolute dating places the site in the Early (Pre-pottery or Aceramic) Neolithic, approximately between 7,700 and 7,100 BCE (Flohr et al., 2020), with a recent radiocarbon date indicating occupation into the early 7th millennium BCE.

Archaeological investigations at Bestansur have been conducted through the excavation of 15 trenches (Supplementary Figure S8), revealing evidence of Early Neolithic occupation over four hectares. These include the remains of permanent mudbrick buildings, work and fire installations, and traces of daily activities (Iversen, 2020a; Matthews et al., 2020b; Richardson et al., 2020). Together with zooarchaeological and archaeobotanical data, these findings suggest year-round habitation, mainly sustained by wild resources from a biodiverse landscape (Bendrey et al., 2020; Matthews et al., 2020c; Whitlam et al., 2020; de Groene et al., 2021, 2023;). The artifactual record of the site is dominated by locally sourced materials, such as clays, stone and freshwater shells from the nearby spring and river, used to produce functional objects and adornments (Matthews et al., 2020d; Mudd, 2020; Richardson, 2020). Materials from distant sources, including marine shells, obsidian and carnelian, are less common but attest to involvement in wide-reaching exchange networks, stretching from the Red Sea to East Anatolia and Iran (Richardson, 2020, 2025).

To date, a minimum of 85 individuals have been recovered from buildings and open spaces across the site (Figure 2c) (Ragazzon, 2025). Mortuary deposits range from single, discrete inhumations to highly commingled, multiple interments, with widespread evidence for the retention, curation and redeposition of skeletal elements (Supplementary Figure S9) (Walsh and Matthews, 2018; Walsh, 2020). The greatest concentration of human remains and objects made from non-local materials has been documented in two elaborate, superimposed buildings, collectively referred to as the Building 5/8 complex (Walsh, 2020). This complex, interpreted as a communal and ceremonial space with mortuary functions, has been linked with social differentiation and the negotiation of collective identities at the site (Matthews et al., 2020d; Richardson et al., 2020)

Variability in mortuary behaviors and the distinctive features of Building 5/8 have led to the hypothesis that Bestansur gathered local and non-local individuals from extended mobility networks. At the same time, zooarchaeological and artifactual evidence suggests that some social segments were periodically mobile, mixing sedentary strategies with logistical forays for resource procurement (Matthews et al., 2020d). The application of laser

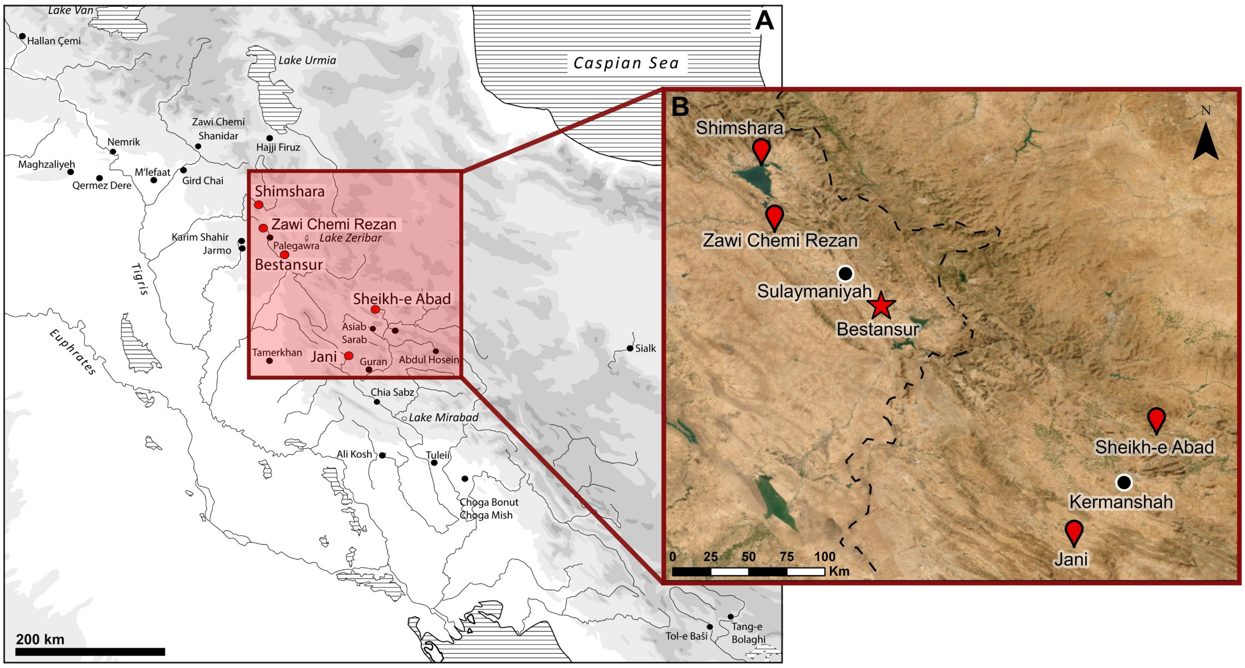

FIGURE 1
(A) Map of Epipalaeolithic and Neolithic sites in the Eastern Fertile Crescent with indication of the study area (shaded in red; image adapted from Matthews et al., 2020a, p. 4); **(B).** Satellite view of the study area showing the location of archaeological sites discussed in the study (red teardrop and star symbols) with respect to the modern cities of Sulaymaniyah and Kermanshah (black circles). The border between Iraq and Iran is marked with a dashed line. Created in ArcGIS Pro v.3.4, using an Earthstar Geographics basemap.

ablation strontium isotope analysis to human remains from the site offers an avenue for exploring and expanding on these ideas, supporting a more nuanced understanding of community dynamics and mobility in an understudied region.

2 Strontium isotope analysis for mobility reconstruction

Strontium isotope analysis relies on the relationship between $^{87}Sr/^{86}Sr$ ratios in dental enamel and those of the local geology at the time of enamel formation (Ericson, 1985). Radiogenic ^{87}Sr, a decay product of the parent isotope rubidium-87 (^{87}Rb), varies relative to stable ^{86}Sr depending on the age and original rubidium content of rocks (Bentley, 2006; Britton, 2020), resulting in different isotopic signatures across different geological substrates. Because of the long half-life of ^{87}Rb (48.8 billion years) (Faure and Mensing, 2005), these signatures remain essentially stable over archaeological time scales. With bedrock weathering, soluble strontium is transferred to soils, water reservoirs and the biosphere (Capo et al., 1998; Flockhart et al., 2015; Britton, 2020). Its bioavailable fraction is then incorporated into the forming enamel of animals and humans as a substitute for calcium, mainly via gastrointestinal absorption from diet and drinking water (Johnson et al., 1966; Apostoaei, 2002). Along this pathway, $^{87}Sr/^{86}Sr$ ratios do not undergo significant fractionation, remaining mostly unaltered from those of the geological source (Bentley, 2006). Therefore, by comparing $^{87}Sr/^{86}Sr$ ratios in dental enamel against baselines for specific areas, it is, in principle, possible to draw inferences about the provenance and mobility of individuals (Montgomery, 2010; Bataille et al., 2020). In practice, however, the level at which movement patterns can be interpreted is contingent upon factors requiring careful consideration. These include the composition of the diet, which may bias $^{87}Sr/^{86}Sr$ ratios toward the origin of high-strontium foods (Lahtinen et al., 2021; Linscott et al., 2023), and the degree of isotopic heterogeneity within the study region.

Establishing baselines that adequately reflect $^{87}Sr/^{86}Sr$ variation in given environments is essential for mobility studies. While bioavailable strontium pools are primarily determined by local lithology, processes like soil mixing, differential mineral weathering, and atmospheric and hydrological inputs can introduce isotopic variability (Bataille et al., 2020; Holt et al., 2021; Spies et al., 2025), which is then transferred to animals through plants and water. To account for these complexities, the selection of baseline archives should be informed by the environmental context of the investigated area (Holt et al., 2021). In general, it has become increasingly common to integrate multiple environmental and faunal proxies to capture broader and more representative $^{87}Sr/^{86}Sr$ ranges (e.g. Al-Shorman et al., 2025; Eckelmann et al., 2025; Goodarzi et al., 2025). Building on these datasets, isotope distribution maps (isoscapes) can further aid mobility tracing and spatial assignment across larger areas. However, the suitability of their use depends on the scale of the study, and is greatest in data-rich regions, where the spatial modeling of $^{87}Sr/^{86}Sr$ ratios is supported by dense background sampling (Bataille et al., 2020).

Because dental enamel forms incrementally and does not remodel after the enamel matrix matures into mineralised tissue

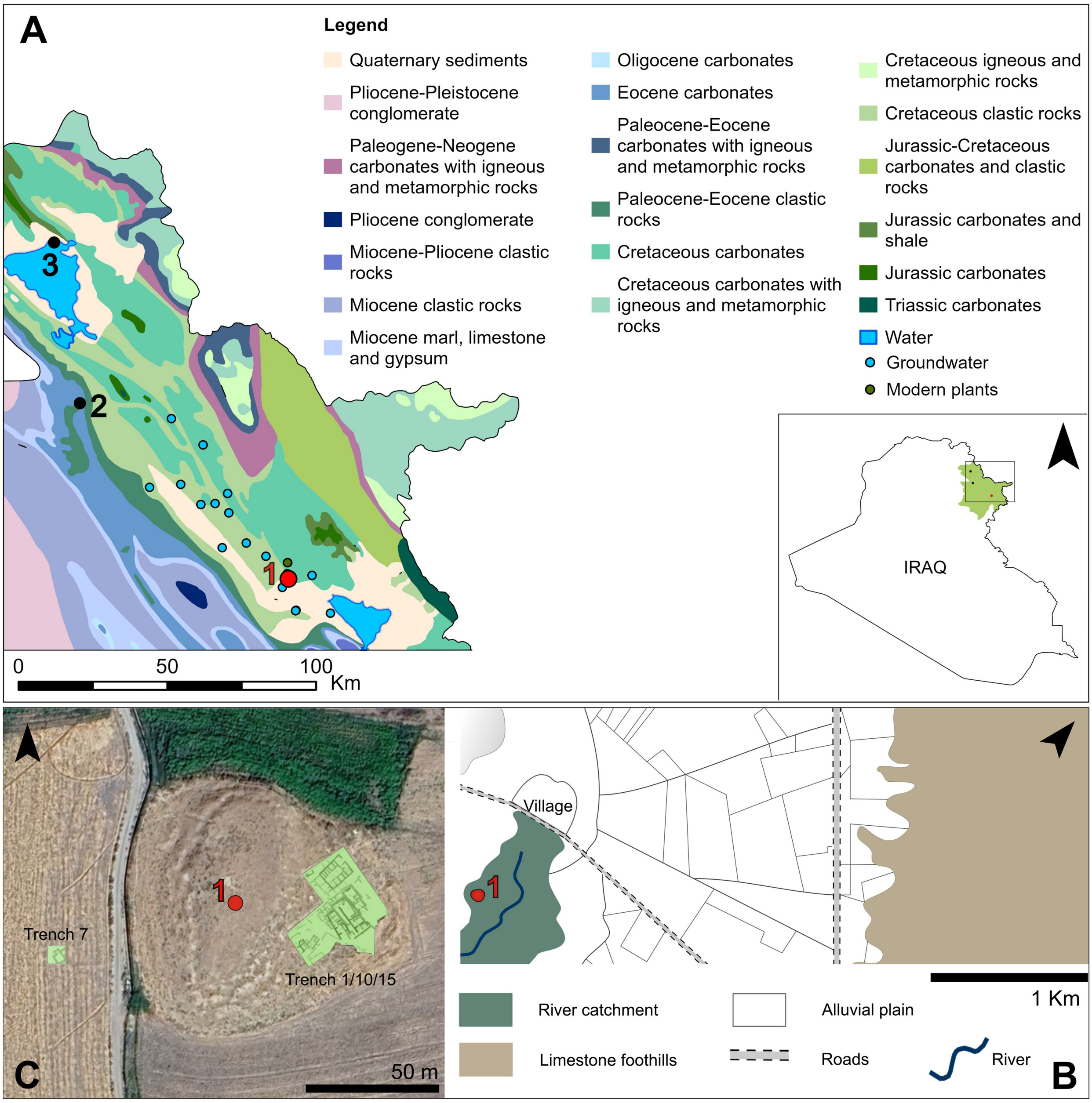

FIGURE 2
(A) Simplified geolithological map of the Sulayimaniyah province of Iraqi Kurdistan, showing the location of analyzed sites in the Iraqi Zagros (1 = Bestansur, the main focus of the study, in red; 2 = Zawi Chemi Rezan; 3 = Shimshara), and of groundwater (Mahmmud et al., 2022) and modern plant samples with published $^{87}Sr/^{86}Sr$ data in proximity to Bestansur (Elliott et al., 2015). See Supplementary Figure S7 for the loction of analyzed sites in the Iranian Zagros. Created in ArcGIS Pro v.3.4, based on the fourth edition of the Geological Map of Iraq (1:1,000,000) (Sissakian and Fouad, 2015) and the second edition of the Geological Map of the Sulaimaniyah quadrangle (1:250,000) (Sissakian and Fouad, 2016); **(B)** Topographical map of Bestansur showing the location of the site in relation to the river catchment, alluvial plains and Zagros limestone foothills. Adapted from Elliott et al. (2020, p. 100); **(C)** Satellite view of Bestansur showing the location of trenches with human remains analyzed in this study. Created in Google Earth Pro.

(Lacruz et al., 2017; Hillson, 2024), it preserves a broadly sequential record of $^{87}Sr/^{86}Sr$ ratio variability during tooth growth. Spatially resolved micro-sampling gives insights into these changes, enabling the detection of fine-scale biogeochemical variations and thereby enhancing temporal resolution beyond what is achievable through bulk strontium isotope analyses. However, interpretations are complicated by an incomplete understanding of physiological variables, including strontium residence time, its mobilization and recycling in the body, and the precise chronology of enamel maturation (Pryor et al., 2020; Boethius et al., 2024; Hillson, 2024; Spies et al., 2025). These factors have raised questions about the extent to which $^{87}Sr/^{86}Sr$ ratios in teeth may be averaged over time. Recent experimental studies have begun to address these concerns, prompting refinements in micro-sampling strategies. In particular, applications of LA-MC-ICP-MS to animals and humans with known movement histories have demonstrated good alignment between laser ablation data and actual mobility patterns (Lazzerini et al., 2021; Boethius et al., 2022; Le Corre et al., 2023; Yang et al., 2025), supporting its increasing use in mobility studies (e.g. Linscott et al., 2023; Kurila et al., 2025; Vaiglova et al., 2025; Zazzo et al., 2025; Wathen-Avila et al., 2025). While techniques such as Thermal Ionization Mass Spectrometry (TIMS) and solution-based multi-collector inductively coupled plasma mass spectrometry (MC-ICP-MS) are reported to yield higher precision (Spies et al., 2025), LA-MC-ICP-MS has proven especially effective in capturing short-term movements when enamel is ablated along the growth axis, from cusp to cemento-enamel junction (Boethius et al., 2024). Targeting enamel regions adjacent to the dentine-enamel junction, which mineralise first and are therefore less temporally averaged than other parts of the crown (Müller et al., 2019), has been proposed to further improve temporal resolution. The time- and cost-efficiency of LA-MC-ICP-MS also facilitates the analysis of multiple sequentially forming teeth per individual (Pryor et al., 2020, 2024a,b), supporting life-course approaches to mobility reconstruction.

At Bestansur, multi-tooth laser ablation strontium isotope analysis was employed to investigate mobility from infancy to late adolescence. In the absence of regional isoscapes or detailed bioavailable strontium isotope records for the Central Zagros, $^{87}Sr/^{86}Sr$ data are integrated with multi-proxy baseline characterization for the site, supplemented by archaeological and bioarchaeological evidence to support interpretations.

3 Materials and methods

3.1 Materials – sediment samples

Sediments analyzed for this study originated from archaeological archive samples kept at the University of Reading and collected during the excavation of Neolithic sites investigated by CZAP in 2008 (Jani and Sheikh-e Abad; Kermanshah Province, Iran), and between 2012 and 2023 (Bestansur, Shimshara and Zawi Chemi Rezan; Sulaymaniyah Province, Iraq). Based on material availability, at least two samples were taken from each site. All archive samples were derived from sealed Neolithic deposits, except for one from Jani and one from Shimshara (JAN2 and SHI1, respectively). These had originally been removed as sediment blocks from sections of the archaeological mounds exposed by water erosion. In the other cases, sample selection targeted clay sediments from occupational layers. An overview of sampling locations and context types is provided in Supplementary Table S6.

3.2 Materials – faunal dental samples

Seven archaeological animal teeth were selected from the Iraqi sites of Bestansur, Zawi Chemi Rezan and Shimshara, complementing sediment analysis for the definition of bioavailable strontium baselines (Supplementary Table S5). Sampling was dictated by material availability but preferentially targeted rodents. Indeed, small mammals with restricted feeding ranges and shorter lifespans are recognized to be better proxies for local strontium bioavailability on circumscribed spatiotemporal scales (Bentley, 2006; Holt et al., 2021; Spies et al., 2025). Samples included three mouse (*Mus*) teeth for Bestansur, and one hare (*Lepus*) and two rabbit (*Oryctolagus*) teeth for Zawi Chemi Rezan. For Shimshara, a single sheep/goat (*Ovis/Capra*) tooth was available for analysis. The seasonal movement and status of ovicaprids at the site are not well established, and evidence for potential management is inconclusive (Bendrey et al., 2020). The inadequate understanding of exploitation regimes and feeding ranges for these herbivores, be they wild, managed or fully domesticated, complicates the *a priori* interpretation of their $^{87}Sr/^{86}Sr$ ranges as local. Indeed, these may reflect averaging of ratios incorporated over large areas (Bataille et al., 2020; Holt et al., 2021). Such interpretative uncertainties were here counterbalanced through the integration of the animal proxy with sediment-derived data.

3.3 Materials – human dental samples

The human dataset included 101 permanent teeth belonging to 41 individuals from Bestansur. To explore variability in provenance and mobility patterns, individuals originating from articulated, disarticulated and mixed, commingled mortuary deposits were sampled from different burial locations across the site. All deposits can be dated to the Neolithic occupation of the site, with most sampled individuals dating back to the mid- to late 8th millennium BCE, and two individuals ascribable to a slightly later chronological horizon (C2387 SK1 and C2387 SK2; early 7th millennium BCE). A plan linking the original location of individuals to available radiocarbon determinations is shown in Figure 3.

Based on previous osteological analyses (see Ragazzon, 2025 for methodological details), sampled individuals ranged from 5 to 45+ years of age and were classified as older children (5.6–10.5 years; $n = 4$), adolescents (10.6–19 years; $n = 9$), young/middle adults (20–40 years; $n = 20$) and mature adults (40+ years; $n = 8$) according to their midpoint age estimate. Biological sex estimates were available for one older child, two adolescents and 23 adults. The older child (C1812 SK9) and one of the adolescents (C1228 SK1) were genetically determined to be male and female, respectively (Lazaridis et al., 2022), while the sex of the second adolescent, aged 16–18 years, was osteologically estimated to be male (C2387 SK2). Due to poor skeletal preservation, confidence in estimates for adults varied considerably, often exhibiting a probabilistic component. Overall, 14 individuals could be classified as females or probable females (F/F?), and nine as males or probable males (M/M?). In six additional cases, biological sex was marked as indeterminate or unknown (ND). For the purpose of this study, females were pooled with probable females, and males with probable males. It is important to stress that the expression "biological sex" is used here to distinguish aspects of anatomical and/or genetic variation from socially constructed gender identities (British Association for Biological Anthropology and Osteoarchaeology, 2022). While biological sex estimates serve as a proxy for accessing diverse experiences in the past, they are employed with an awareness of the limitations of bioarchaeological methods, which do not fully capture the broad range of human variation.

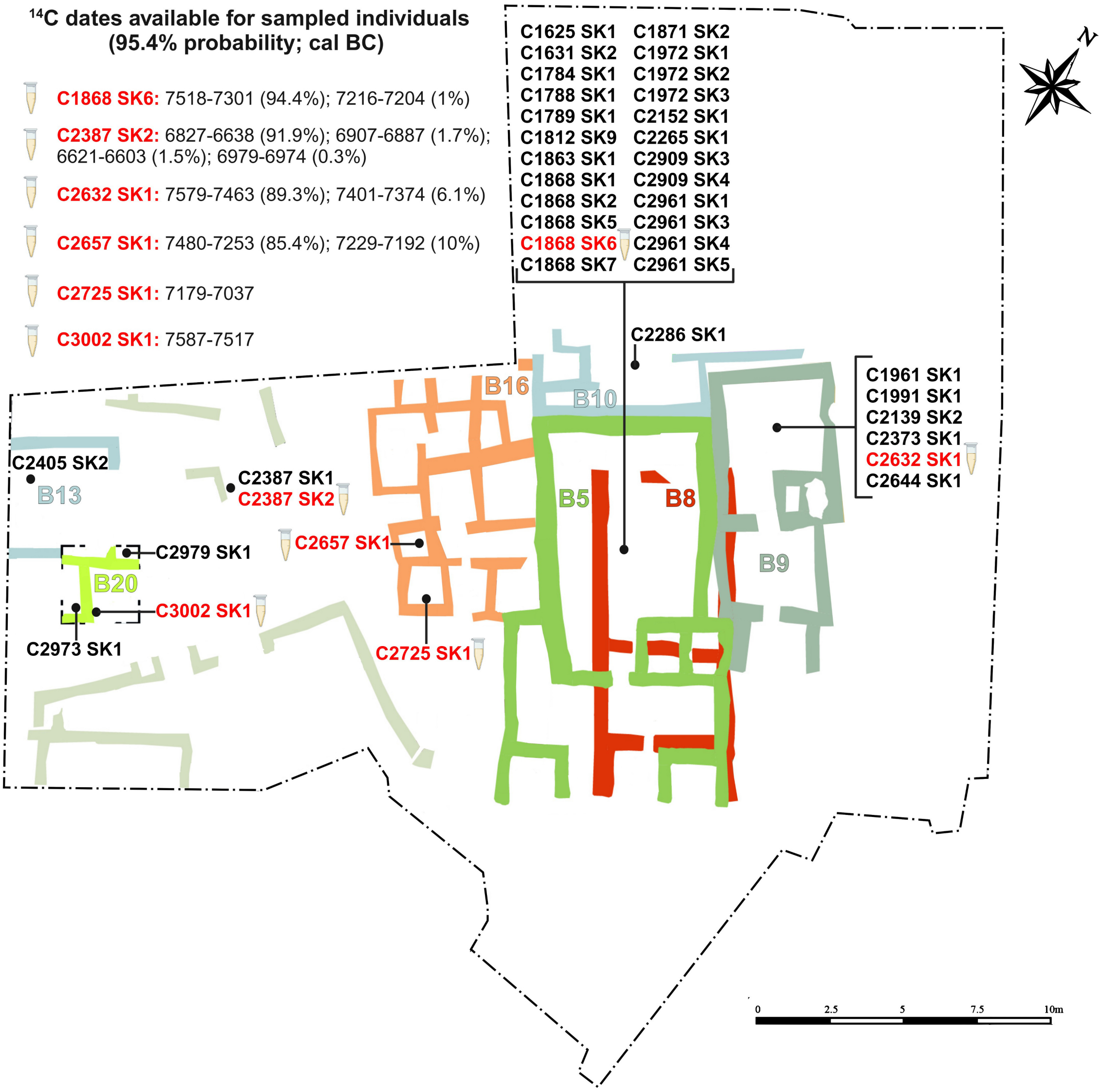

FIGURE 3
Bestansur; plan of Trench 10 and Trench 1/15 showing the distribution of individuals included in the study, with indication of those with available 14C dates (in red). Radiocarbon data are derived from Flohr et al. (2020) and Matthews et al. (in preparation). ©CZAP. Created in BioRender (https://BioRender.com/l8le9t3).

To support a life-course approach to the exploration of mobility, sample selection fell on the first (M1), second (M2) and third (M3) molars, teeth whose sequential formation spans infancy to adolescence (AlQahtani et al., 2010). Individuals preserving M1, M2 and M3s were preferentially sampled, as this allowed for greater temporal depth in analysis. Indeed, based on median development stages, crown formation takes place approximately between 4.5 months and 3.5 years for M1s, 2.5 and 8.5 years for M2s, and 8.5 and 14.5 years for M3s (AlQahtani et al., 2010), although M3s are reportedly characterized by greater developmental variability (Hillson, 2024). A few individuals presenting only one (M1 or M2) or two (e.g. M1 and M2 or M2 and M3 pairs) of the selected teeth were also included to increase representativeness. Further sampling criteria are detailed in Supplementary Text S3, while a complete list of human dental samples is provided in Supplementary Table S7.

3.4 Preparation and analysis of sediment samples using TIMS

The preparation and analysis of sediment samples were carried out at the National Center for Isotope Geochemistry at University College Dublin (Dublin, Ireland). Eleven sediment samples of approximately 8.5 g each were leached in 30 ml of ultrapure water (18.2 MΩ-cm) (Linscott et al., 2023) and agitated three times a day for 15 days. After filtration of the leach solutions, two 1 ml aliquots were collected for each sample. One aliquot was run on a Thermo Scientific iCAP Q quadrupole ICP-MS instrument to measure strontium concentrations. The second aliquot was further processed to determine $^{87}Sr/^{86}Sr$ bioavailability.

Aliquots to be analyzed for $^{87}Sr/^{86}Sr$ were transferred to columns with ~100 µl of SR-Spec resin (Triskem, France), and strontium was separated following procedures modified after

Pin et al. (1994). Collected strontium samples and blanks were dried on a hot plate until full evaporation of the liquid fraction (~24 hours), before dilution in 10 μl of 0.05 M HNO3 and loading of 1 μl onto a rhenium filament (99.99%, H.Cross) with 1 μl of TaCl5 activator solution. Strontium isotope measurements were performed on a Thermo Scientific Triton Thermal Ionization Mass Spectrometer on Faraday cups in static mode with amplifier rotation. Instrument performance and analytical accuracy were monitored with the SRM987 isotopic standard, which yields $^{87}Sr/^{86}Sr = 0.710266 \pm 0.000022$ (2σ, $n = 21$). The ratio recorded on the day of the analytical session was 0.710264. Mass fractionation was corrected with an exponential law normalized to $^{86}Sr/^{88}Sr = 0.1194$. Interference from ^{87}Rb on ^{87}Sr was monitored using ^{85}Rb and was negligible in all cases. Contribution from a procedural blank of ~2,200 pg was also negligible.

3.5 Preparation and analysis of dental samples using LA-MC-ICP-MS

Sample collection and preparation for human and animal teeth was carried out in the chemistry laboratory at the Department of Archaeology and History, University of Exeter (Exeter, UK). Following the protocol described in Pryor et al. (2020), slices of enamel and adhering dentine of approximately 2–3 mm in thickness were cut from dental crowns, from the cusp to the cemento-enamel junction, using a diamond-tipped circular saw. This approach keeps destruction to a minimum and enables the preservation of most of the tooth for future analyses. Rodent teeth were cut either longitudinally or, for very small teeth, transversely, to create slices exposing a cross-section through the enamel. Both human and faunal dental slices were embedded in Epofix© epoxy resin then sanded with 35 μm and 15.3 μm grit papers until attainment of a flat, polished surface.

The measurement of strontium isotope ratios took place at the National Oceanography Center, University of Southampton (Southampton, UK), using LA-MC-ICP-MS, with a Thermo Scientific Neptune MC-ICP mass spectrometer coupled to a New Wave 193-nm Ar-F excimer laser ablation system (UP193FX). The laser track was set to target enamel close to the enamel-dentine junction, from cusp to cementoenamel junction. Additionally, dentine was analyzed along randomly placed 1–4 mm lines in a subsample of five human teeth to cross-reference ratios with those obtained from sediments and faunal samples. The enamel and dentine targeted for analysis were cleaned with the laser, and data were then collected using the following analytical settings: laser beam diameter at 110 μm, 15 Hz repetition rate and either 10, 15 or 20 $\mu m/s^{-1}$ translation rate depending on the length of the profile being measured. The ablated material was transferred from the laser cell to the MC-ICP-MS using a He carrier gas which was then mixed with Ar and N_2 before injection into the plasma ion source. $^{87}Sr/^{86}Sr$ measurements were taken in static collection mode with a set integration time of 1.049 s, and the instrumental setup was tuned for the minimization of oxide production, monitored as $^{254}(UO)+/^{238}U+$, following Lewis et al. (2014).

After the analysis, masses were corrected to an on-peak gas blank for ^{86}Kr interference. Subsequently, ratios underwent correction for mass fractionation using an exponential law (Russell et al., 1978) normalized to $^{86}Sr/^{88}Sr = 0.1194$ (Nier, 1938). Rare earth element contamination was assessed using yttrium-89 (^{89}Y) as a proxy, with datapoints presenting anomalously high ^{89}Y concentrations discarded as diagenetically altered (Woodhead et al., 2005). The isobaric interference of ^{87}Rb on ^{87}Sr was also corrected to the natural $^{87}Rb/^{85}Rb$ ratio of 0.385617 (de Laeter et al., 2003). Calcium dimers and argides in carbonate materials are known to have only a negligible effect on measured $^{87}Sr/^{86}Sr$ ratios, however their impact on $^{84}Sr/^{86}Sr$ ratios is significant (Woodhead et al., 2005). We therefore corrected $^{84}Sr/^{86}Sr$ ratios using mass 82 for the ^{40}Ca (or ^{40}Ar)$^{42}Ca+$ molecular ion, followed by a mass balance correction using the natural abundance ratios for calcium (Wieser et al., 2004). This enabled the use of the reported $^{84}Sr/^{86}Sr$ ratios as a quality control against the accepted value of 0.0565 (Woodhead et al., 2005). For each analytical session, accuracy and reproducibility were tested through repeat measurement of an in-house enamel standard obtained from pigs fed a controlled marine diet (Lewis et al., 2017), with $^{87}Sr/^{86}Sr$ pre-characterized to 0.709076 using thermal ionization mass spectrometry (TIMS). Repeat analyses of the standard across three analytical sessions ($n = 29$) gave a mean of 0.709127 ± 0.000193 (2σ), equating to a mean positive offset of 71 ± 273 parts per million (ppm; 2σ) for LA-MC-ICP-MS over TIMS.

3.6 Sampling rights and permissions

Sediment, animal and human samples from Iraq and Iran were exported and analyzed with permission from the Slemani Directorate of Antiquities and Heritage (Kurdistan Regional Government, Iraq), and the Iranian Center for Archaeological Research (Iranian Culture, Heritage and Tourism Organization, Iran), respectively. All research activities on organic and inorganic materials from the sites included in the study were conducted with the authorization of the relevant excavation directors and approved by the host institutions.

4 Results

4.1 Local baselines for Bestansur and other Central Zagros sites

In this study, the concept of "local" was defined as encompassing Bestansur and its primary source area for water, food, and construction materials, namely the karst spring and river catchment in which the site is located, as well as the surrounding alluvial plain up to the Zagros foothills, within a radius of approximately 2.5–3 km (Figure 2b). While this spatial definition is relatively narrow, it reflects the current distribution of baseline samples and, based on contextual evidence, it should be regarded as a conservative minimum estimate of the area regularly used by individuals for basic resource procurement. A local baseline of bioavailable strontium was established by combining $^{87}Sr/^{86}Sr$ ratios from archaeological sediment leachates from the site (0.70794–0.70812; $n = 3$), rodent enamel (0.70800–0.70819; $n = 2$) and dentine also from the site (0.70798–0.70815; $n = 2$) (Supplementary Tables S2, S5–S6), and published modern plants collected from the mound and surrounding fields (0.70815–0.70816; $n = 3$; Supplementary Table S1) (Elliott et al., 2015). Human dentine samples yielded consistently higher $^{87}Sr/^{86}Sr$ ratios (0.70832–0.70854; $n = 4$) and were thus excluded from baseline calculations (see expanded discussion in Supplementary Text S2, 3, Figures S5, 6 and Table S3).

Based on the minimum and maximum ratios covered by all baseline proxies, the lower and upper bounds of the local $^{87}Sr/^{86}Sr$ range were set at 0.70794 and 0.70819, respectively. In terms of surficial geology, all microfaunal and environmental samples originated from the archaeological mound and the surrounding fields, which lie on a Cretaceous clastic substrate, overlain by Quaternary alluvial deposits in places. The baseline range is therefore likely to reflect mixed inputs from Quaternary alluvium, Cretaceous clastic rocks and pelagic limestone (Saeed Ali, 2007; Elliott et al., 2015), with groundwater from the spring contributing averaged $^{87}Sr/^{86}Sr$ signals from multiple Cretaceous-age geological formations (Shiranish, Tanjero, Kometan and Balambo) (Saeed Ali, 2007). Ratios fall largely within the 0.7076–0.7082 range reported for groundwater samples from 16 water wells within a maximum radius of 70 km from the site (Figure 2a), where small $^{87}Sr/^{86}Sr$ variability has been attributed to the dominant influence of Cretaceous carbonate dissolution (Mahmmud et al., 2022). Strontium isotope ratios reported for two modern plant specimens sampled on the limestone foothills of the Zagros, approximately 3 km away from Bestansur, overlap with the site baseline, corresponding to 0.70795 and 0.70803 (Elliott et al., 2015).

Fewer archival proxies were available for the other Central Zagros sites (Supplementary Tables S5, 6). In the Iraqi Zagros, sediment leachates ($n = 2$) and sheep/goat dentine ($n = 1$) from Shimshara, which is located on a conglomerate outcrop capped by Quaternary alluvium, yielded a narrow range of 0.70790–0.70801. This expands slightly to 0.70781–0.70824 when enamel $^{87}Sr/^{86}Sr$ ratios from same ovicaprine tooth are considered. At Zawi Chemi Rezan, which sits on an Eocene carbonate bedrock, sediment samples ($n = 2$), and rodent enamel ($n = 3$) and dentine ($n = 1$) produced ratios between 0.70803 and 0.70832. In the Iranian Zagros, sediment leachates yielded $^{87}Sr/^{86}Sr$ ratios of 0.70822 ± 0.00003 and 0.70825 ± 0.00002 ($n = 2$) for Jani and 0.70829 ± 0.00002 for Sheikh-e Abad ($n = 2$), both located on Quaternary alluvial deposits (Supplementary Figure S7). Overall, variation is low across sites, and ratios fall within indicative $^{87}Sr/^{86}Sr$ ranges for the isotopic zones proposed by Lü et al. (2023), namely the Iranian plateau (0.7075–0.7090) and the Iraqi foothills of the Zagros (0.7080–0.7085).

4.2 Laser ablation $^{87}Sr/^{86}Sr$ data for Bestansur human enamel

Sequential $^{87}Sr/^{86}Sr$ profiles for 101 human teeth (38 first, 38 s and 25 third molars) representing 41 individuals from Bestansur are presented in Supplementary Figures S10–13. Contextual information about sampled teeth and summary statistics for the entire dataset are provided in Supplementary Tables S4 and S7, respectively. Strontium isotope ratios for dental enamel range from 0.70773 to 0.70856.

Enamel $^{87}Sr/^{86}Sr$ profiles show strong alignment with the site baseline across the dataset. Intra-tooth $^{87}Sr/^{86}Sr$ variability, calculated as the range between maximum and minimum ratios, is low across the sample, spanning 0.00012 to 0.00068 (Figure 4). The most homogenous profiles are observed in the molars of two mature adult (probable) females, C2286 SK1 and C3002 SK1, while the largest variation is noted in the second molar of a young/middle adult female, C1788 SK1 (Figure 5). Comparisons by biological sex and burial location reveal similar intra-tooth $^{87}Sr/^{86}Sr$ variability between the teeth of females ($n = 34$; 0.00012–0.00068) and males ($n = 25$; 0.00021–0.00058), and those of individuals interred within Building 5/8 ($n = 59$; 0.00021–0.00068) and at other locations ($n = 42$; 0.00012–0.00052).

Despite general consistency with the baseline, repeated intra-tooth fluctuations toward more and less radiogenic ratios are observed across several $^{87}Sr/^{86}Sr$ profiles (Figure 5). At the same time, a few teeth fall completely or largely above the local range. These include the first and second molars of a mature adult of indeterminate sex (C2632 SK1) and the second molar of a young/middle adult female (C2909 SK3). In individual C2909 SK3, a shift toward higher ratios is already apparent in the last third of the $^{87}Sr/^{86}Sr$ profile for the first molar. Two additional individuals, C2286 SK1 and C3002 SK1, have profiles plotting mostly above the baseline, though they cluster very close to its upper bound. Except for the first molar of C2632 SK1, all teeth display at least some overlap with the local range. Although mobility remains a plausible interpretation for individuals showing the highest and lowest ratios, profile deviations from the range defined as "local" fall largely within the 2σ analytical uncertainty of laser ablation measurements. Their interpretation as non-local signals therefore cannot be made with confidence.

All individuals with unworn first molars ($n = 6$), where enamel loss is negligible, and which are therefore expected to best capture the earliest phase of cusp mineralisation, exhibit ratios that are broadly consistent with, or only slightly more radiogenic than the local range in the initial section of their $^{87}Sr/^{86}Sr$ profiles. The terminal sections of profiles from non-adult teeth whose crowns were still forming at the time of death and are thus likely to reflect their last place of residence ($n = 7$), also fall within the baseline or cluster close to its upper bound. Beyond C2909 SK3, there is no evidence for marked changes in $^{87}Sr/^{86}Sr$ catchments between the mineralisation of the first, second and third molars, that is, between infancy, childhood and adolescence, in individuals with multiple teeth available for analysis.

5 Discussion

5.1 Strontium isotope variability and the definition of local baselines in the Central Zagros

Environmental and faunal baseline proxies from five Neolithic sites in the Central Zagros yielded $^{87}Sr/^{86}Sr$ ratios between

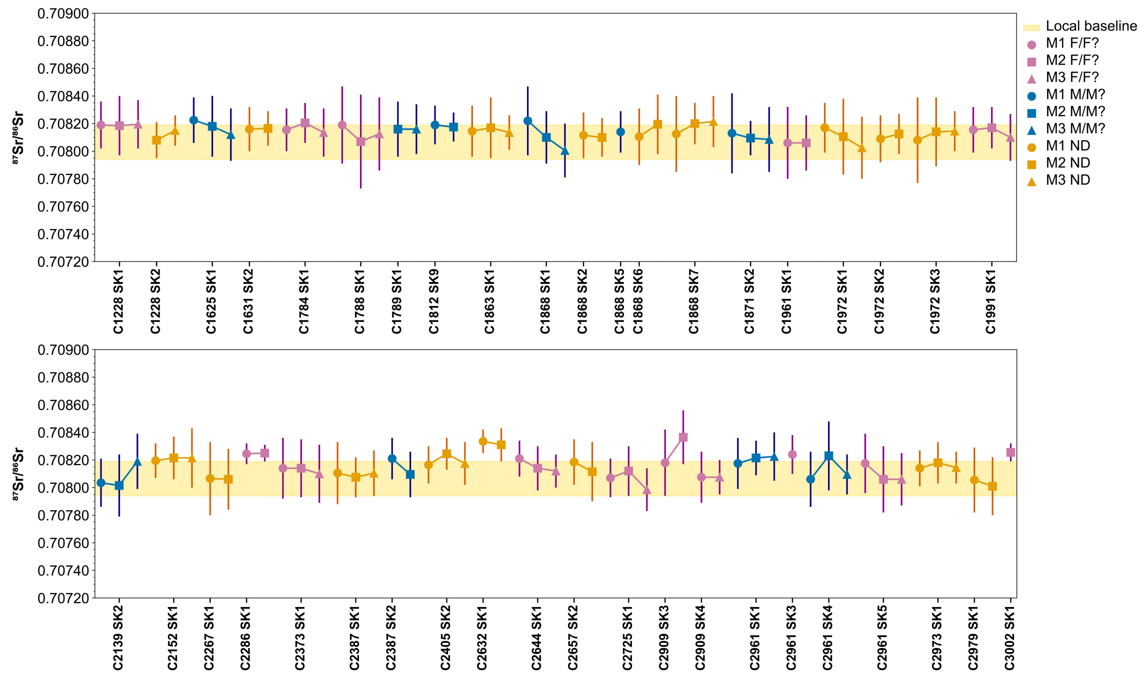

FIGURE 4
Floating bar chart representing a summary of $^{87}Sr/^{86}Sr$ data for human enamel samples from Bestansur. Individual bars represent $^{87}Sr/^{86}Sr$ ranges as defined by the minimum and maximum ratios for each tooth (based on a 20-point running average of individual laser ablation measurements). Circle, square and triangle markers indicate the central point of each range, identifying teeth as first, second or third molars. Color denotes sex. The local baseline for the site is represented as a yellow band in the background.

0.70794 and 0.70832, largely within the predictive range proposed by Lü et al. (2023) for the Zagros foothills. While samples for Shimshara, Zawi Chemi Rezan, Jani and Sheikh-e-Abad were limited in number, offering only a preliminary characterization of local strontium bioavailability, their analysis indicates low inter-site $^{87}Sr/^{86}Sr$ variability. This is partly due to similarities in geolithological substrates within a landscape dominated by carbonates. However, the small range of $^{87}Sr/^{86}Sr$ ratios even where surficial geologies apparently differ, as at the Iraqi sites, suggests an additional influence of specific environmental factors and geomorphic processes. Proximity to water and extensive alluviation are correlated with differential weathering and the mixing of strontium from multiple sources (Bentley, 2006), potentially resulting in dampened $^{87}Sr/^{86}Sr$ variability. Although groundwater is generally expected to have a limited impact on bioavailable strontium pools (Holt et al., 2021), in the Zagros, where karst aquifers provide one of the main water sources (Mustafa et al., 2016; Mahmmud et al., 2022), it likely plays a non-negligible role. At Bestansur, for example, local isotopic averaging may have been shaped by the position of the site within the catchment of the perennial spring and spring-fed river, which supplied water, clay for construction and fertile soils for plants exploited during the Neolithic. This apparent homogeneity, however, should not be assumed to characterize the whole region, and particularly non-settled areas where mixing processes may be less pronounced. In the Sulaymaniyah province, geolithological variation is seen within a minimum radius of 20 to 50 km from the sites analyzed (Figure 2a), and some degree of $^{87}Sr/^{86}Sr$ variability may be expected across yet-unsampled substrates.

Based on the marine strontium isotope curve, which reflects $^{87}Sr/^{86}Sr$ variation in seawater over the geologic time scale (McArthur et al., 2020), ratios dropped to minima below 0.7070 during the Middle/Upper Jurassic and steadily increased above 0.7085 from the Middle Miocene. The $^{87}Sr/^{86}Sr$ ratios of marine carbonates dating to these periods can thus be expected to mirror negative and positive shifts in the curve slope, influencing bioavailable $^{87}Sr/^{86}Sr$ ranges. When taking Bestansur as a reference point, Middle/Upper Jurassic and Neogene geologies are found ~20 km to the north-east and ~25 km to the west, respectively. Further distinctive $^{87}Sr/^{86}Sr$ ranges may be found in areas where carbonates interact with volcanic rocks. One such area is the Mawat district, ~100 km to the north, where whole-rock $^{87}Sr/^{86}Sr$ ratios of 0.7057–0.7067 are reported for mafic rocks and andesites (Koyi, 2009; Aswad et al., 2014). The Penjween district, ~40 km north-east of the site, may also exhibit different $^{87}Sr/^{86}Sr$ ranges due to the contribution of mafic and felsic rocks ($^{87}Sr/^{86}Sr$ = 0.7031–0.7074) (Abdulzahra et al., 2018; Azizi et al., 2025) to bioavailable strontium pools. While this study had to rely on existing archival collections for the analysis of environmental proxies, additional fine-scale sampling will be required to refine the characterization of $^{87}Sr/^{86}Sr$ distribution across the region.

5.2 Community make-up, residential stability and logistical mobility at Bestansur

Laser ablation strontium isotope analysis at Bestansur provides new insights into human mobility and the emergence

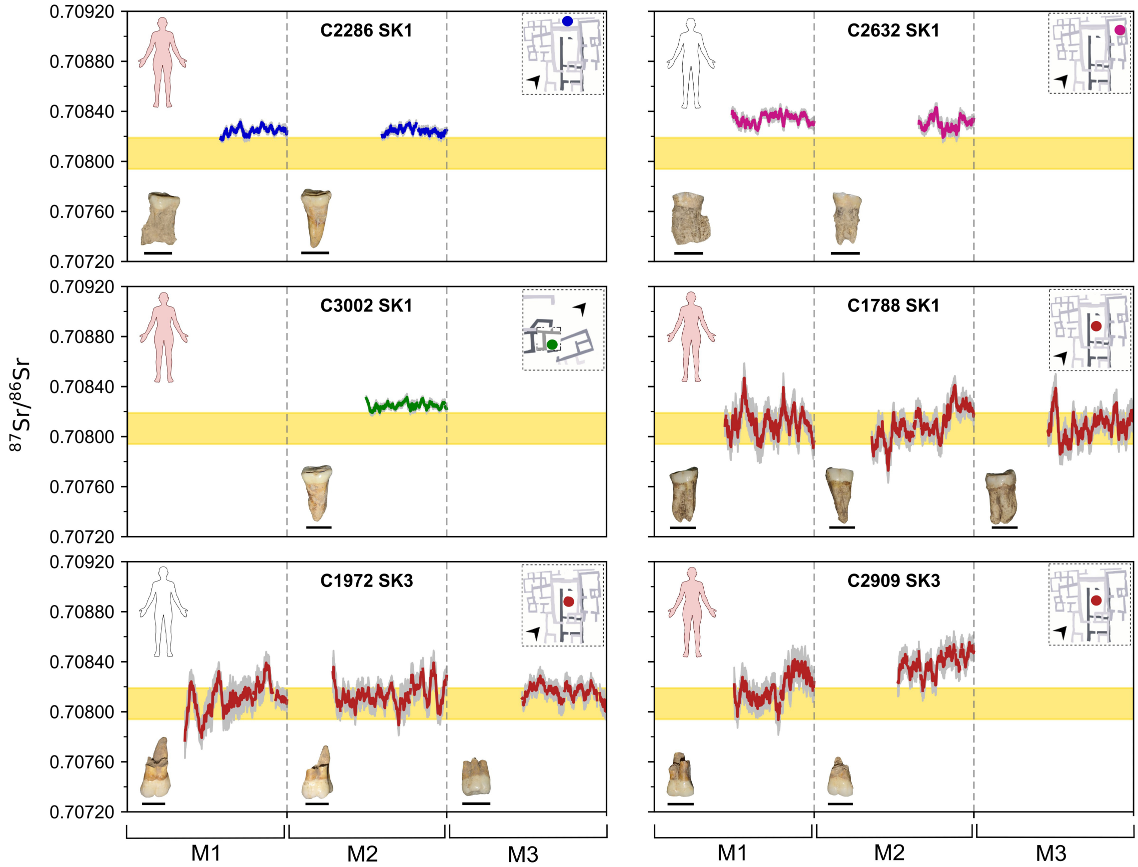

FIGURE 5
Laser ablation strontium isotope profiles for the first (M1), second (M2) and third molars (M3) of six individuals from Bestansur (C2286 SK1, C2632 SK1, C3002 SK1, C1788 SK1, C1972 SK3 and C2909 SK3). Lines represent the 20-point running average of individual laser ablation measurements and are colored according to burial location. Blue (top left plot) indicates Building 10, fuchsia (top right plot) indicates Building 9, green (mid left plot) indicates Building 20, and red (remaining plots) indicates Building 5/8 (see also Figure 3 and Supplementary Table S7). Gray shading around these lines indicates the standard error, while the local baseline for the site is represented as a yellow band in the background. Profiles for all the analyzed individuals are given in Supplementary Figures S10–13. Estimated biological sex is shown in the top left corner of each plot (red figure = female/probable female; white figure = indeterminate/unknown sex). Created in BioRender (https://BioRender.com/5e6zsph).

of sedentism in the Central Zagros. When considering the first molars ($n = 38$), which mineralise during infancy, a single mature adult of indeterminate sex (C2632 SK1) had a $^{87}Sr/^{86}Sr$ profile plotting entirely above the baseline (0.70825–0.70840), consistent with a possible non-local origin. Two mature adult females (C2286 SK1 and C3002 SK1) also exhibited $^{87}Sr/^{86}Sr$ profiles largely above the baseline, though repeatedly overlapping with the local range. For all three individuals, deviations from the baseline fall within the 2σ analytical uncertainty for laser ablation measurements, making their identification as possible non-locals tenuous. All other teeth displayed broad alignment with the baseline, indicating a predominantly local make-up of the Bestansur community. Because the sample includes individuals spanning childhood to mature adulthood, this pattern of locality may have extended across multiple generations.

Adherence to the baseline from the first through the third molars further suggests commitment to the site throughout non-adult life. A single young/middle adult female (C2909 SK3) may have spent part of their childhood in a different geological setting, as suggested by an extended shift in strontium catchments between the first and second molar. However, the deviation from the baseline in the second molar is inconsistent across the $^{87}Sr/^{86}Sr$ profile, indicating either intermittent interactions with the site or movement within areas characterized by similar bioavailable strontium pools. Overall, the close correspondence between $^{87}Sr/^{86}Sr$ ratios and the local range in unworn first molars and molars still forming at the time of death is compatible with the individuals having been born, lived, and died at the site or in its immediate surroundings. The paucity of mobility data for the Central Zagros and the Eastern Fertile Crescent limits the contextualization of Bestansur within broader regional frameworks. At the contemporary site of Ali Kosh, in the Iranian Zagros, strontium isotope data suggest greater mobility (Darabi et al., 2024). Conversely, individuals from Nemrik, in the Upper Tigris valley, have provisionally been interpreted as local based on strontium and oxygen isotope analyses (Ávila et al., 2026). Mobility reconstructions at these sites are currently constrained by the preliminary nature of investigations and small sample sizes (seven individuals at Ali Kosh and two at Nemrik; Darabi et al., 2024; Ávila et al., 2026). Nevertheless, they point to some contextual variability in mobility patterns during the 8th millennium BCE, highlighting the need for larger datasets to support robust interpretations of regional trends in human movement.

At Bestansur, no clear patterns of $^{87}Sr/^{86}Sr$ variability can be identified based on biological sex, burial location or type of mortuary deposit (e.g. articulated vs. disarticulated; single vs. multiple individuals). Comparable isotope studies focusing on Neolithic Southwest Asia report no clear associations between provenance and mortuary treatment, attributing this to processes of integration and constructed affiliation that rendered non-locals and locals archaeologically indistinguishable (Pearson et al., 2023; Wang et al., 2023b; Plug et al., 2025). The picture emerging from the site broadly agrees with this interpretation, suggesting that mortuary practices were shaped by roles, statuses and identities acquired during life, and/or by mourning behaviors negotiated by the living (Croucher, 2012, 2018), rather than by the individuals' origins.

At present, enamel $^{87}Sr/^{86}Sr$ data is not sufficient to support the identification of Bestansur as a supra-local aggregation center drawing people from the wider region, although convergence from isotopically indistinguishable landscapes cannot be excluded. When integrated with archaeological evidence, $^{87}Sr/^{86}Sr$ data indicate ties between the analyzed individuals and the site locales that transcend short-term place connections. Hallmarks of sedentism include the construction, maintenance, and renovation of permanent buildings, as well as continued mortuary activities binding the sphere of the living to that of the dead (Matthews et al., 2020b; Richardson et al., 2020). The presence of synanthropic rodents linked to food storage and waste-management practices, and the seasonality of exploited animal taxa, including birds, can be interpreted as additional indicators of year-round habitation (Tchernov, 1991; Bendrey et al., 2020). Residential stability at Bestansur was likely sustained by increased water availability during the Early Holocene (Regattieri et al., 2023; Rostami et al., 2024) and by resource accessibility in a favorable environment. In this context, $^{87}Sr/^{86}Sr$ data from the site align with archaeological evidence for the establishment of increasingly permanent settlements in the region during the 8th millennium BCE (Zeder, 2024a). Beyond the Zagros, the results of this study echo isotope analyses from other sites across Southwest Asia, which also reveal predominantly local community make-ups and strong commitment to places during the Early Neolithic (Alt et al., 2013; Benz et al., 2016a,b; Santana et al., 2021; Pearson et al., 2023; Wang et al., 2023b).

Alongside the increasing adoption of sedentary lifeways, the period spanning the 9th to the 7th millennium BCE is associated with an intensification of cross-regional interactions in Southwest Asia (Watkins, 2023). The material culture of Bestansur reflects such connections: objects made of obsidian, carnelian and marine shells point to contacts stretching from the Sinai to Anatolia and Iran, and from the Persian Gulf to the Red Sea and the Eastern Mediterranean (Richardson, 2020, 2025). The exact modalities through which these networks were maintained, however, are difficult to reconstruct. One reason is that extended mobility undertaken by adults who grew up at Bestansur, left the site and later returned to be buried would remain invisible in the strontium isotope record, which only captures non-adult residence. Although some children may have participated in extended mobile behaviors, as possibly suggested for individual C2909 SK3, evidence for this is weak. Interpretations are also complicated by overlaps between the $^{87}Sr/^{86}Sr$ range for the site and those of many contemporary contexts across Southwest Asia (Santana et al., 2021; Pearson et al., 2023; Wang et al., 2023a,b; Darabi et al., 2024; Giaccari et al., 2025; Plug et al., 2025), limiting the ability of biogeochemical analyses to confidently detect episodes of long-distance mobility. Notably, however, non-local materials are far less common than utilitarian and decorative objects made with resources from the nearby springhead and Zagros limestone outcrops (Matthews et al., 2020d; Mudd, 2020; Richardson, 2020). Estimates of obsidian movement into the site likewise indicate relatively modest volumes of traffic, not supporting intensive or highly organized exchanges (Matthews et al., 2020d). Instead, these data appear more consistent with episodic interactions, in which materials reached the site through multi-step circulation and/or mobility by select individuals, rather than large-scale engagement in long-distance movements.

While cross-regional mobility in Southwest Asia may be challenging to explore using $^{87}Sr/^{86}Sr$ data, repeated intra-individual fluctuations in $^{87}Sr/^{86}Sr$ ratios within and across teeth require consideration. Except for two mature adult females with highly homogeneous profiles (C2286 SK1 and C3002 SK1), reflecting consistent strontium sourcing during infancy and childhood, several individuals exhibit $^{87}Sr/^{86}Sr$ ratios that oscillate above and below the local baseline, spanning approximately 0.70773–0.70856. Because the timing of enamel mineralisation, strontium residence in the body and dietary equilibration all act to average $^{87}Sr/^{86}Sr$ ratios (Pryor et al., 2020; Boethius et al., 2022), these fluctuations are indicative of marked and/or prolonged shifts in dietary strontium sourcing, sufficient to produce detectable variation in enamel profiles. These may be linked with the exploitation of bioavailable strontium pools within and, possibly, outside of the local catchment, as consistent with episodes of short-term mobility away from the site. Lower $^{87}Sr/^{86}Sr$ ratios are compatible with contributions from ubiquitous Upper Cretaceous carbonates, which have reportedly low whole-rock ratios (0.70764–0.70796 for dolomites in the Zagros basin) (Mansurbeg et al., 2021), as well as from Middle/Upper Jurassic carbonates, which dominate the landscape 20 km north-east of Bestansur. Conversely, endmembers with higher $^{87}Sr/^{86}Sr$ ratios are more difficult to pinpoint without more extensive characterization of the regional isoscape. These may tentatively be identified with Middle Miocene and Pliocene substrates located ∼25 km to the west, in the biodiverse area of the Qara Dagh mountains. It must be emphasized, however, that the observed fluctuations in $^{87}Sr/^{86}Sr$ profiles are small, limiting confidence in inferring mobility beyond the site locales. Interpretations are further constrained by the lack of dense background sampling in the area surrounding Bestansur and the broader region, which makes it difficult to exclude the impact of minor isotopic heterogeneity within homogenous geological settings. Additional fine-scale baseline mapping will be required to better understand micro-scale strontium isotope variability and refine the provisional interpretations presented here.

Ethnoarchaeological research suggests that when residential mobility decreases in foraging communities, logistical mobility increases to ensure continued access to a wide pool of resources (Binford, 1980; Kelly, 2013). At Bestansur, zooarchaeological and archaeobotanical evidence indicates strong reliance on wild foods within a hybrid, low-level food production economy (Bendrey et al., 2020; Iversen, 2020b; Whitlam et al., 2020; de Groene et al., 2021, 2023), implying that logistical movements may have been periodically required to meet the needs of the community. Preliminary carbon and nitrogen stable isotope analyses of human bone collagen delineate a C_3 terrestrial diet ($n = 7$; $\delta^{13}C = -19.9 \pm 0.2‰$; $\delta^{15}N = 7.1 \pm 0.5‰$). When compared to available baseline values for pigs ($n = 4$; $\delta^{13}C = -20.0 \pm 0.6‰$; $\delta^{15}N = 6.1 \pm 0.6‰$), as well as medium-large herbivores, including sheep/goats ($n = 3$; $\delta^{13}C = -19.3‰$; $\delta^{15}N = 5.4‰$), deer ($n = 1$; $\delta^{13}C = -19.7‰$; $\delta^{15}N = 6.8‰$) and cattle ($n = 1$; $\delta^{13}C = -20.3‰$; $\delta^{15}N = 5.9‰$), human $\delta^{15}N$ values reflect trophic offsets well below the 3–5‰ expected for the regular consumption of these animals (Bocherens and Drucker, 2003). This suggests that animal protein from these species contributed only minimally to human diet. Conversely, the high frequencies of caries recorded at the site are consistent with reliance on plant foods rich in fermentable carbohydrates and, possibly, starches (Ragazzon et al., in preparation). In terrestrial ecosystems, plants contain higher strontium concentrations than meat (Sillen and Kavanagh, 1982; González-Weller, 2013), meaning that the $^{87}Sr/^{86}Sr$ ratios of the consumer will be biased toward the ratios of plant foods. Zooarchaeological, micromorphological and artifactual evidence also demonstrates the consumption of molluscs and freshwater fish at Bestansur (Bendrey et al., 2020; Iversen, 2020b; Mudd, 2020), both resources that can be rich in strontium (Schroeder et al., 1972; Schoeninger and Peebles, 1981; Lahtinen et al., 2021). Although plant foods may have offered lower caloric returns than large game, their accessibility and storability likely made them dietary staples, complemented by the regular exploitation of aquatic resources. As major contributors to human $^{87}Sr/^{86}Sr$ ratios, these foods would have made enamel ratios particularly sensitive to shifts in foraging locales, especially since plants more closely reflect local strontium bioavailability (Bentley, 2006).

While strontium isotope data are not, by themselves, conclusive, their integration with contextual information about the site and its economy enables cautious interpretations. In particular, it can be speculated that intra-individual fluctuations in $^{87}Sr/^{86}Sr$ profiles may reflect non-adults periodically accessing resources from different foraging locales, possibly through active involvement in logistical forays. Although their spatial extent cannot be determined, these activities could have reasonably expanded the resource base available at Bestansur and in its immediate catchment. Participation may have included children accompanying caregivers on foraging activities during the breastfeeding period and early childhood, and later acting as independent food collectors (Lew-Levy et al., 2017). In modern hunter-gatherer groups, adults and children often operate within coordinated and partially overlapping foraging radii, with non-adults fulfilling a substantial portion of their own food requirements (Kelly, 2013). This scenario is broadly consistent with bioarchaeological evidence for the participation of children in subsistence and occupational activities at the site (Walsh, 2022; Ragazzon, 2025). Taken together, biogeochemical and contextual data may therefore be compatible with the inhabitants of the site engaging in targeted logistical movements to secure resources, leaving subtle isotopic traces of a mobile foraging component within otherwise sedentary lifeways. Given the analytical limitations of the dataset, these reconstructions remain tentative; nevertheless, they offer a plausible perspective on patterns of mobility and resource use.

In summary, laser ablation strontium isotope analysis delineates the Bestansur community as largely local, with multi-generational ties to the site. Since excavations are still ongoing, earlier, more mobile phases may remain unidentified. Nevertheless, biogeochemical data, architectural continuity and markers of year-round habitation indicate residential stability during the 8th millennium BCE. While a strong commitment to the site may have been maintained at least throughout non-adult life, it is likely that mobility retained a key role. Small quantities of imported materials suggest episodic cross-regional exchanges, while subtle shifts in $^{87}Sr/^{86}Sr$ profiles across several analyzed teeth might reflect the exploitation of different foraging locales. Based on current knowledge of the economy of Bestansur, foraging activities would have contributed to sustaining an early settled community that was still largely reliant on wild plants and animals. By integrating isotopic data with contextual evidence and ethnoarchaeological parallels, this study offers new insights into emerging sedentism and community structure in the Early Neolithic Central Zagros. Beyond Bestansur, it contributes to the characterization of regional bioavailable strontium isotope variability, offering a framework for further discussions of mobility, landscape use and associated interpretative challenges in Early Neolithic Southwest Asia.

Data availability statement

The original contributions presented in the study are included in the article/Supplementary material, further inquiries can be directed to the corresponding author.

Ethics statement

Ethical approval was not required for the analysis of human or animal samples included in this study, as these are archaeological in nature (older than 100 years). The study was conducted in accordance with the local legislation, institutional requirements and ethical guidelines. All human samples were obtained from archaeological excavations in Iraqi Kurdistan and were exported and analyzed with permission from the Slemani Directorate of Antiquities and Heritage (Kurdistan Regional Government, Iraq). Research activities were conducted with the authorization of the excavation directors and approved by the host institutions. Due to the archaeological nature of the material, written informed consent to participate in this study was not required.

Author contributions

GR: Conceptualization, Data curation, Formal analysis, Funding acquisition, Investigation, Methodology, Project administration, Software, Validation, Visualization, Writing – original draft, Writing – review & editing. RM: Resources, Supervision, Writing – review & editing. JM: Methodology, Software, Validation, Writing – review & editing. DA: Methodology, Software, Validation, Writing – review & editing. KR: Resources, Writing – review & editing. AP: Conceptualization, Investigation, Methodology, Supervision, Validation, Visualization, Writing – review & editing.

Funding

The author(s) declared that financial support was received for this work and/or its publication. This study was supported by the Arts and Humanities Research Council through the South, West and Wales Doctoral Training Partnership, and conducted in the framework of the Central Zagros Archaeological Project (CZAP; AHRC grant AH/H034315/2 2011–2014) and the ERC project 'Middle East Neolithic Transition: Integrated Community Approaches' (MENTICA; ERC AdG 787264). Funding for strontium isotope analysis was obtained through a dedicated research grant from the British Institute for the Study of Iraq.

Acknowledgments

We are extremely grateful to the Slemani Directorate of Antiquities and Heritage (Kurdistan Regional Government, Iraq) and the Iranian Center for Archaeological Research (Iranian Culture, Heritage and Tourism Organization, Iran) for granting permission to access and export the samples analyzed in this study. Major assistance was provided by Kamal Rasheed Raheem and Hussain Gharib of the Slemani Directorate of Antiquities and Heritage, and Professor Hassan Fazeli Nashli of the University of Tehran, for which we are very grateful. We thank Dr Wendy Matthews (University of Reading) for providing access to sediment samples, Professor Alan Outram (University of Exeter) and Dr Gwendoline Maurer (University of Cardiff) for aiding with the identification of animal teeth, Dr Amy Richardson (University of Reading) for sharing site plans and geospatial data for the CZAP sites, Dr Teimoor Nazari-Dehkordi (UCD) for sharing geological maps of Iran, and Amy Collins (University of Exeter) for helping with faunal sample preparation. Special acknowledgments are also due to Varoujan Sissakian for sharing high-resolution geological maps of Iraq, and to Adriaan Prins for his assistance with ArcGIS and the design of Figure 2a and Supplementary Figure S7. We are grateful to The British Institute for the Study of Iraq, whose support made this study possible. Finally, we thank the Editor and the Reviewers for their insightful feedback, which substantially strengthened the manuscript.

Conflict of interest

The author(s) declared that this work was conducted in the absence of any commercial or financial relationships that could be construed as a potential conflict of interest.

Generative AI statement

The author(s) declared that generative AI was not used in the creation of this manuscript.

Any alternative text (alt text) provided alongside figures in this article has been generated by Frontiers with the support of artificial intelligence and reasonable efforts have been made to ensure accuracy, including review by the authors wherever possible. If you identify any issues, please contact us.

Publisher's note

All claims expressed in this article are solely those of the authors and do not necessarily represent those of their affiliated organizations, or those of the publisher, the editors and the reviewers. Any product that may be evaluated in this article, or claim that may be made by its manufacturer, is not guaranteed or endorsed by the publisher.

Supplementary material

The Supplementary Material for this article can be found online at: https://www.frontiersin.org/articles/10.3389/fearc.2026.1818214/full#supplementary-material

References

Abdulzahra, I. K., Hadi, A., Asahara, Y., Azizi, H., and Yamamoto, K. (2018). Petrogenesis and geochronology of Mishao peraluminous I-type granites, Shalair valley area, NE Iraq. *Geochem.* 78, 215–227. doi: 10.1016/j.chemer.2018.01.003

AlQahtani, S. J., Hector, M. P., and Liversidge, H. M. (2010). Brief communication: the London atlas of human tooth development and eruption. *Am. J. Phys. Anthropol.* 142, 481–490. doi: 10.1002/ajpa.21258

Al-Shorman, A., Perry, M., and Coleman, D. (2025). Ancient mobility in northern Jordan during the Roman and Byzantine periods using stable strontium isotope analysis of human dental enamel. *J. Archaeol. Sci. Rep.* 61:104879. doi: 10.1016/j.jasrep.2024.104879

Alt, K. W., Benz, M., Müller, W., Berner, M. E., Schultz, M., Schmidt-Schultz, T. H., et al. (2013). Earliest evidence for social endogamy in the 9,000-year-old-population of Basta, Jordan. *PLoS ONE* 8:e65649. doi: 10.1371/journal.pone.0065649

Altınışık, N. E., Kazanci, D. D., Aydogan, A., Gemici, H. C., Erdal, Ö. D., Sarialtun, S., et al. (2022). A genomic snapshot of demographic and cultural dynamism in upper mesopotamia during the neolithic transition. *Sci. Adv.* 8:eabo3609. doi: 10.1126/sciadv.abo3609

Apostoaei, A. I. (2002). Absorption of strontium from the gastrointestinal tract into plasma in healthy human adults. *Health phys.* 83, 56–65. doi: 10.1097/00004032-200207000-00006

Aswad, K. J., Al-Samman, A. H., Aziz, N. R., and Koyi, A. M. (2014). The geochronology and petrogenesis of Walash volcanic rocks, Mawat nappes: constraints on the evolution of the northwestern Zagros suture zone, Kurdistan Region, Iraq. *Arab. J. Geosci.* 7, 1403–1432. doi: 10.1007/s12517-013-0873-x

Ávila, J. N., Sołtysiak, A., Austin, C., Darabi, H., Leonard, N. D., Nashli, H.F, et al. (2026). Seasonality and water source strategies in the Neolithic Near East (ca. 8,000–5,000 BCE): Insights from multi-proxy isotopic and elemental analyses. *J. Archaeol. Sci.* 186:106462. doi: 10.1016/j.jas.2025.106462

Azizi, H., Yara, I., Ali, S. A., Mohammad, Y. O., Asahara, Y., Minami, M., et al. (2025). The Penjween gabbro, Northeastern Iraq, revealing a forearc hyperextension regime with a slow spreading ridge center in the Late Cretaceous. *Geochem.* 85:126241. doi: 10.1016/j.chemer.2024.126241

Bataille, C. P., Crowley, B. E., Wooller, M. J., and Bowen, G. J. (2020). Advances in global bioavailable strontium isoscapes. *Palaeogeogr. Palaeoclimatol. Palaeoecol.* 555:109849. doi: 10.1016/j.palaeo.2020.109849

Bendrey, R., Van Neer, W., Bailon, S., Rofes, J., Herman, J., Morlin, M., et al. (2020). “Animal remains and human-animal-environment relationships at Early Neolithic Bestansur and Shimshara” in *The Early Neolithic of the Eastern Fertile Crescent: Excavations at Bestansur and Shimshara, Iraqi Kurdistan*, eds. R. Matthews, W. Matthews, K.R. Raheem and A. Richardson (Oxford: Oxbow Books), 311–352.

Bentley, R. A. (2006). Strontium isotopes from the Earth to the archaeological skeleton: a review. *J. Archaeol. Method Theory* 13, 135–187. doi: 10.1007/s10816-006-9009-x

Benz, M., Erdal, Y. S., Sahin, F.S., Özkaya, V., and Alt, K.W. (2016a). “The equality of inequality. Social differentiation among the hunter-fisher-gatherer community of Körtik Tepe, Southeastern Turkey” in *Rich and poor–competing for resources in Prehistory. 8th Archaeological Conference of Central Germany. October 22–24, 2015 in Halle (Saale)*, eds. H.H. Meller, H.P. Hahn, R. Jung and R. Risch (Halle: Landesamt für Denkmalpflege und Archäologie Sachsen-Anhalt) 147–164.

Benz, M., Sahin, F. S., Erdal, Y. S., and Özkaya, V. (2016b). Results of stable isotopes from Kortik Tepe Southeastern Turkey. *Arkeometri Sonuçlari Toplantisi* 31, 231–252.

Binford, L. R. (1980). Willow smoke and dogs’ tails: hunter-gatherer settlement systems and archaeological site formation. *Am. Antiq.* 45, 4–20. doi: 10.2307/279653

Bocherens, H., and Drucker, D. (2003). Trophic level isotopic enrichment of carbon and nitrogen in bone collagen: case studies from recent and ancient terrestrial ecosystems. *Int. J. Osteoarchaeol.* 13, 46–53. doi: 10.1002/oa.662

Boethius, A., Ahlström, T., Kielman-Schmitt, M., Kjällquist, M., and Larsson, L. (2022). Assessing laser ablation multi-collector inductively coupled plasma mass spectrometry as a tool to study archaeological and modern human mobility through strontium isotope analyses of tooth enamel. *Archaeol. Anthropol. Sci.* 14:97. doi: 10.1007/s12520-022-01556-9

Boethius, A., Storå, J., Gustavsson, R., and Kielman-Schmitt, M. (2024). Mobility among the stone age island foragers of Jettböle, Åland, investigated through high-resolution strontium isotope ratio analysis. *Quat. Sci. Rev.* 328:108548. doi: 10.1016/j.quascirev.2024.108548

British Association for Biological Anthropology and Osteoarchaeology. (2022). *BABAO Statement on Sex Estimation.* Available online at: https://babao.org.uk/babao-statement-on-sex-estimation/ (Accessed October 15, 2025).

Britton, K. (2020). “Isotope analysis for mobility and climate studies” in *Archaeological Science: an Introduction,* eds. M.P. Richards and K. Britton (Cambridge: Cambridge University Press) 99–124.

Broushaki, F., Thomas, M. G., Link, V., López, S., Van Dorp, L., Kirsanow, K., et al. (2016). Early Neolithic genomes from the Eastern Fertile Crescent. *Science* 353, 499–503. doi: 10.1126/science.aaf7943

Capo, R. C., Stewart, B. W., and Chadwick, O. A. (1998). Strontium isotopes as tracers of ecosystem processes: theory and methods. *Geoderma* 82, 197–225. doi: 10.1016/S0016-7061(97)00102-X

Croucher, K. (2012). *Death and Dying in the Neolithic Near East*. Oxford: Oxford University Press. doi: 10.1093/acprof:osobl/9780199693955.001.0001

Croucher, K. (2018). Keeping the dead close: Grief and bereavement in the treatment of skulls from the Neolithic Middle East. *Mortality* 23, 103–120. doi: 10.1080/13576275.2017.1319347

Daly, K. G., Mattiangeli, V., Hare, A. J., Davoudi, H., Fathi, H., Doost, S. B., et al. (2021). Herded and hunted goat genomes from the dawn of domestication in the Zagros Mountains. *Proc. Natl. Acad. Sci. U.S.A.* 118:e2100901118. doi: 10.1073/pnas.2100901118

Darabi, H. (2022). The creative millennia: highlighting the transitional neolithic (ca. 9800-8000 BCE) in the Central Zagros, Iran. *J. Archaeol. Sci.* 14, 37–58.

Darabi, H., Richter, T., Sołtysiak, A., Arranz-Otaegui, A., Davoudi, H., and Nishiaki, Y. (2024). Revisiting Neolithic Ali Kosh: new insights into settlement sustainability, human mobility, and subsistence strategies. *J. Field Archaeol.* 49, 527–546. doi: 10.1080/00934690.2024.2382012

de Groene, D., Bendrey, R., and Matthews, R. (2021). Pigs in the neolithic of the Eastern fertile crescent: new evidence from pre-pottery Neolithic Bestansur and Shimshara, Iraqi Kurdistan (7800–7100 BC). *Int. J. Osteoarchaeol.* 31:1258–1269. doi: 10.1002/oa.3035

de Groene, D., Bendrey, R., Müldner, G., Coogan, A., and Matthews, R. (2023). Sheep and goat management in the Early Neolithic in the Zagros region (8000–5000 BC): new zooarchaeological and isotopic evidence from Ganj Dareh, Bestansur and Jarmo. *J. Archaeol. Sci. Rep.* 49:103936. doi: 10.1016/j.jasrep.2023.103936

de Laeter, J. R., Böhlke, J. K., de Bièvre, P., Hidaka, H., Peiser, H. S., Rosman, K. J. R., et al. (2003). Atomic weights of the elements. Review 2000 (IUPAC Technical Report). *Pure Appl. Chem.* 75, 683–800. doi: 10.1351/pac200375060683

Dow, G. K., and Reed, C. G. (2015). The Origins of sedentism: climate, population, and technology. *J. Econ. Behav. Organ.* 119, 56–71. doi: 10.1016/j.jebo.2015.07.007

Eckelmann, R., Arppe, L., Tarasov, A., Pospieszny, Ł., Ackerman, L., Heyd, V., et al. (2025). Mobility and community at Mesolithic Lake Onega, Karelia, north-west Russia: insights from strontium isotope analysis. *Archaeol. Anthropol. Sci.* 17:17. doi: 10.1007/s12520-024-02129-8

Elliott, S., Bendrey, R., Whitlam, J., and Aziz, K. R. (2020). “Ethnoarchaeological research in Bestansur: insights into vegetation, land-use, animals and animal dung” in *The Early Neolithic of the Eastern Fertile Crescent: Excavations at Bestansur and Shimshara, Iraqi Kurdistan*, eds. R. Matthews, W. Matthews, K.R. Raheem and A. Richardson (Oxford: Oxbow Books) 91–106.

Elliott, S., Bendrey, R., Whitlam, J., Aziz, K. R., and Evans, J. (2015). Preliminary ethnoarchaeological research on modern animal husbandry in Bestansur, Iraqi Kurdistan: Integrating animal, plant and environmental data. *Environ. Archaeol.* 20, 283–303. doi: 10.1179/1749631414Y.0000000025

Ericson, J. E. (1985). Strontium isotope characterization in the study of Prehistoric human ecology. *J. Hum. Evol.* 14, 503–514. doi: 10.1016/S0047-2484(85)80029-4

Faure, G., and Mensing, T. M. (2005). *Isotopes: principles and applications*. Hoboken: John Wiley and Sons.

Flockhart, D. T., Kyser, T. K., Chipley, D., Miller, N. G., and Norris, D. R. (2015). Experimental evidence shows no fractionation of strontium isotopes (^{87}Sr/^{86}Sr) among soil, plants, and herbivores: Implications for tracking wildlife and forensic science. *Isot. Environ. Health Stud.* 51, 372–381. doi: 10.1080/10256016.2015.1021345

Flohr, P., Matthews, R., Matthews, W., Richardson, A., and Fleitmann, D. (2020). “Radiocarbon dating of Bestansur and Shimshara” in *The Early Neolithic of the Eastern Fertile Crescent: Excavations at Bestansur and Shimshara, Iraqi Kurdistan*, eds. R. *Matthews, W.* Matthews, K.R. Raheem and A. Richardson (Oxford: Oxbow Books) 187–196.

Giaccari, M., Romano, L., D’Agostino, F., and Tafuri, M. A. (2025). DATAMESOP: DATAset on stable isotope measurement (Strontium, Oxygen and Carbon) of archaeological and non-archaeological materials from South-West Asia for MESOPotamia. *J. Open Archaeol. Data.* 13, 1–6. doi: 10.5334/joad.152

González-Weller, D., et al. (2013). Dietary intake of barium, bismuth, chromium, lithium, and strontium in a Spanish population (Canary Islands, Spain). *Food Chem. Toxicol.* 62, 856–868. doi: 10.1016/j.fct.2013.10.026

Goodarzi, P., Dehpahlavan, M., and Sołtysiak, A. (2025). Settled farmers or mobile herders? *Patterns of mobility at Shahr-i Qumis, a late antiquity site in northern Iran, investigated using strontium isotope values. Archaeol. Anthropol. Sci.* 17:39. doi: 10.1007/s12520-024-02150-x

Gregoricka, L. A. (2021). Moving forward: a bioarchaeology of mobility and migration. *J. Archaeol. Res.* 29, 581–635. doi: 10.1007/s10814-020-09155-9

Hillson, S. (2024). *Dental anthropology*. Cambridge: Cambridge University Press.

Holt, E., Evans, J. A., and Madgwick, R. (2021). Strontium (^{87}Sr/^{86}Sr) mapping: a critical review of methods and approaches. *Earth-Sci. Rev.* 216:103593. doi: 10.1016/j.earscirev.2021.103593

Iversen, I. (2020a). “Microarchaeology: The small traces of Neolithic activities” in *The Early Neolithic of the Eastern Fertile Crescent: Excavations at Bestansur and Shimshara, Iraqi Kurdistan*, eds. R. Matthews, W. Matthews, K.R. Raheem and A. Richardson (Oxford: Oxbow Books) 287–310.

Iversen, I. (2020b). “Bestansur molluscs: Regional context and local activities” in *The Early Neolithic of the Eastern Fertile Crescent: Excavations at Bestansur and Shimshara, Iraqi Kurdistan,* eds. R. Matthews, W. Matthews, K.R. Raheem and A. Richardson (Oxford: Oxbow Books*)* 397–410.

Johnson, A. R., Armstrong, W. D., and Singer, L. (1966). Strontium incorporation into dental enamel. *Science* 153, 1396–1397. doi: 10.1126/science.153.3742.1396

Kelly, R. L. (2013). *The lifeways of hunter-gatherers: The foraging spectrum*. Cambridge: Cambridge University Press.

Knipper, C., Gresky, J., and Benz, M. (2023). “Local people or masked mobility: Results of strontium isotope analysis of human teeth” in *Death in Ba’ja: Sepulchral identity and symbolism in an Early Neolithic community of the Transjordanian Highlands.*

Household and Death in Ba'ja 2, eds. M. Benz, J. Gresky, C. Purschwitz and H.G.K. Gebel (Heidelberg: Propylaeum) 291–307.

Koyi, A. M. (2009). Sr-Nd isotopical significance of Walash volcanic rocks, Mawat area, NE Iraq. *ZJPAS* 21, 39–45.

Kurila, L., Piličiauskiene, G., Simčenka, E., Lidén, K., Kooijman, E., and Miliauskiene, Ž. (2025). Late Roman and Migration Period elites from Lithuania–locals or migrants? Reinterpretation of the current concept based on $^{87}Sr/^{86}Sr$ stable isotope analysis. *Archaeol. Anthropol. Sci.* 17:35. doi: 10.1007/s12520-024-02151-w

Lacruz, R. S., Habelitz, S., Wright, J. T., and Paine, M. L. (2017). Dental enamel formation and implications for oral health and disease. *Physiol. Rev.* 97, 939–993. doi: 10.1152/physrev.00030.2016

Lahtinen, M., Arppe, L., and Nowell, G. (2021). Source of strontium in archaeological mobility studies—marine diet contribution to the isotopic composition. *Archaeol. Anthropol. Sci.* 13:1. doi: 10.1007/s12520-020-01240-w

Lazaridis, I., Alpaslan-Roodenberg, S., Acar, A., Açikkol, A., Agelarakis, A., Aghikyan, L., et al. (2022). The genetic history of the Southern Arc: a bridge between West Asia and Europe. *Science* 377: eabm4247.

Lazaridis, I., Nadel, D., Rollefson, G., Merrett, D. C., Rohland, N., Mallick, S., et al. (2016). Genomic insights into the origin of farming in the ancient Near East. *Nature* 536, 419–424. doi: 10.1038/nature19310

Lazzerini, N., Balter, V., Coulon, A., Tacail, T., Marchina, C., Lemoine, M., et al. (2021). Monthly mobility inferred from isoscapes and laser ablation strontium isotope ratios in caprine tooth enamel. *Sci. Rep.* 11:2277. doi: 10.1038/s41598-021-81923-z

Le Corre, M., Grimes, V., Lam, R., and Britton, K. (2023). Comparison between strip sampling and laser ablation methods to infer seasonal movements from intra-tooth strontium isotopes profiles in migratory caribou. *Sci. Rep.* 13:3621. doi: 10.1038/s41598-023-30222-w

Lewis, J., Coath, C. D., and Pike, A. W. G. (2014). An improved protocol for $^{87}Sr/^{86}Sr$ by laser ablation multi-collector inductively coupled plasma mass spectrometry using oxide reduction and a customised plasma interface. *Chem. Geol.* 390, 173–181. doi: 10.1016/j.chemgeo.2014.10.021

Lewis, J., Pike, A. W., Coath, C. D., and Evershed, R. P. (2017). Strontium concentration, radiogenic ($^{87}Sr/^{86}Sr$) and stable ($\delta^{88}Sr$) strontium isotope systematics in a controlled feeding study. *STAR* 3, 45–57. doi: 10.1080/20548923.2017.1303124

Lew-Levy, S., Reckin, R., Lavi, N., Cristóbal-Azkarate, J., and Ellis-Davies, K. (2017). How do hunter-gatherer children learn subsistence skills? *A meta-ethnographic review. Hum. Nat.* 28, 367–394 doi: 10.1007/s12110-017-9302-2

Linscott, B., Pike, A. W., Angelucci, D. E., Cooper, M. J., Milton, J. S., Matias, H., et al. (2023). Reconstructing Middle and Upper Paleolithic human mobility in Portuguese Estremadura through laser ablation strontium isotope analysis. *Proc. Natl. Acad. Sci. U.S.A.* 120:e2204501120. doi: 10.1073/pnas.2204501120

Lü, Q. Q., Chen, Y. X., Henderson, J., and Bayon, G. A. (2023). A large-scale Sr and Nd isotope baseline for archaeological provenance in silk road regions and its application to plant-ash glass. *J. Archaeol. Sci.* 149:105695. doi: 10.1016/j.jas.2022.105695

Mahmmud, R., Sracek, O., Mustafa, O., Cejková, B., Jačková, I., and Vondrovicová, L. (2022). Groundwater geochemistry evolution and geogenic contaminants in the Sulaimani-Warmawa Sub-basin, Kurdistan Region, Iraq. *Environ. Monit. Assess.* 194:352. doi: 10.1007/s10661-022-09933-6

Mansurbeg, H., Alsuwaidi, M., Salih, N., Shahrokhi, S., and Morad, S. (2021). Integration of stable isotopes, radiometric dating and microthermometry of saddle dolomite and host dolostones (Cretaceous carbonates, Kurdistan, Iraq): new insights into hydrothermal dolomitization. *Mar. Pet. Geol.* 127:104989. doi: 10.1016/j.marpetgeo.2021.104989

Matthews, R., Matthews, W., Richardson, A., and Raheem, K. R. (2020a). "The Neolithic transition in the Eastern Fertile Crescent: Project themes, aims and objectives" in *The Early Neolithic of the Eastern Fertile Crescent: Excavations at Bestansur and Shimshara, Iraqi Kurdistan*, eds. R. Matthews, W. Matthews, K.R. Raheem and A. Richardson (Oxford: Oxbow Books), 1–18.

Matthews, R., Richardson, A., and Maeda, O. (2020d). "Early Neolithic chipped stone worlds of Bestansur and Shimshara" in *The Early Neolithic of the Eastern Fertile Crescent: Excavations at Bestansur and Shimshara, Iraqi Kurdistan*, eds. R. Matthews, W. Matthews, K.R. Raheem and A. Richardson (Oxford: Oxbow Books) 461–532.

Matthews, W., García-Suárez, A., Portillo, M., Speed, C., Allistone, G., Bull, I., et al. (2020b). "Integrated micro-analysis of the built environment and resource use: High-resolution microscopy and geochemical, mineralogical, phytolith and biomolecular approaches" in *The Early Neolithic of the Eastern Fertile Crescent: Excavations at Bestansur and Shimshara, Iraqi Kurdistan*, eds. R. Matthews, W. Matthews, K.R. Raheem and A. Richardson (Oxford: Oxbow Books), 265–286.

Matthews, W., Matthews, R., Richardson, A., and Raheem, K. R. (2020c). "The Neolithic transition in the Eastern Fertile Crescent: thematic synthesis and discussion" in *The Early Neolithic of the Eastern Fertile Crescent: Excavations at Bestansur and Shimshara, Iraqi Kurdistan*, eds. R. Matthews, W. Matthews, K.R. Raheem and A. Richardson (Oxford: Oxbow Books), 623–656.

McArthur, J. M., Howarth, R. J., Shields, G. A., and Zhou, Y. (2020). "Strontium isotope stratigraphy" in *Geologic time scale 2020*, eds. F. Gradstein, J.G., Ogg, M.D. Schmitz and G.M. Ogg (Amsterdam: Elsevier) 211–238.

Montgomery, J. (2010). Passports from the past: Investigating human dispersals using strontium isotope analysis of tooth enamel. *Ann. Hum. Biol.* 37, 325–346. doi: 10.3109/03014461003649297

Mudd, D. (2020). "Ground stone tools and technologies" in *The Early Neolithic of the Eastern Fertile Crescent: Excavations at Bestansur and Shimshara, Iraqi Kurdistan*, eds. R. Matthews, W. *Matthews, K.R. Raheem and A. Richardson (Oxford: Oxbow Books)* 567–612.

Müller, W., Nava, A., Evans, D., Rossi, P. F., Alt, K. W., and Bondioli, L. (2019). Enamel mineralization and compositional time-resolution in human teeth evaluated via histologically-defined LA-ICPMS profiles. *Geoch. Cosm. Acta* 255, 105–126. doi: 10.1016/j.gca.2019.03.005

Mustafa, O., Tichomirowa, M., Kummer, N. A., and Merkel, B. (2016). Assessment of water-rock interaction processes in the Karst Springs of Makook Anticline (Kurdistan Region, Iraq) using Sr-isotopes, rare earth, and trace elements. *Arab. J. Geosci.* 9:368. doi: 10.1007/s12517-016-2344-7

Nier, A. O. (1938). The isotopic constitution of strontium, barium, bismuth, thallium and mercury. *Phys. Rev.* 54:275. doi: 10.1103/PhysRev.54.275

Pearson, J., Evans, J., Lamb, A., Baird, D., Hodder, I., Marciniak, A., et al. (2023). Mobility and kinship in the world's first village societies. *Proc. Natl. Acad. Sci. U.S.A.* 120: e2209480119. doi: 10.1073/pnas.2209480119

Pin, C., Briot, D., Bassin, C., and Poitrasson, F. (1994). Concomitant separation of strontium and samarium-neodymium for isotopic analysis in silicate samples, based on specific extraction chromatography. *Anal. Chim. Acta* 298, 209–217. doi: 10.1016/0003-2670(94)00274-6

Plug, J. H., Blevins, K. E., Abbès, F., Akkermans, P. M., Bach Gómez, A. M., Chambrade, M. L., et al. (2025). Strontium and oxygen isotope analysis reveals changing connections to place and group membership in the world's earliest village societies. *Sci. Rep.* 15:34598. doi: 10.1038/s41598-025-18134-3

Pryor, A. J. E., Ameen, C., Liddiard, R., Baker, G., Kanne, K. S., Milton, J. A., et al. (2024b). Isotopic biographies reveal horse rearing and trading networks in medieval London. *Sci. Adv.*, 10: eadj5782. doi: 10.1126/sciadv.adj5782

Pryor, A. J. E., Insoll, T., and Evis, L. (2020). Laser ablation strontium isotope analysis of human remains from Harlaa and Sofi, Eastern Ethiopia, and the implications for Islamisation and mobility. *STAR* 6, 113–136. doi: 10.1080/20548923.2020.1843266

Pryor, A. J. E., Nesnídalová, T., Šída, P., Lengyel, G., and Standish, C. D., Milton, J.A. (2024a). Reindeer prey mobility and seasonal hunting strategies in the late Gravettian mammoth steppe. *Archaeol. Anthropol. Sci.* 16:123. doi: 10.1007/s12520-024-02019-z

Ragazzon, G. (2025). External auditory exostoses in fragmentary remains: Evidence for activity and human-environment interactions at Early Neolithic Bestansur, Iraqi Kurdistan. *Int. J. Paleopathol.* 51, 43–54. doi: 10.1016/j.ijpp.2025.09.003

Regattieri, E., Forti, L., Drysdale, R. N., Mannella, G., Hellstrom, J. C., Conati Barbaro, C., et al. (2023). Neolithic hydroclimatic change and water resources exploitation in the Fertile Crescent. *Sci. Rep.* 13:45. doi: 10.1038/s41598-022-27166-y

Richardson, A. (2020). "Material culture and networks of Bestansur and Shimshara" in *The Early Neolithic of the Eastern Fertile Crescent: Excavations at Bestansur and Shimshara, Iraqi Kurdistan*, eds. R. Matthews, W. Matthews, K.R. Raheem and A. Richardson (Oxford: Oxbow Books) 533–566.

Richardson, A. (2025). Networks of knowledge, materials, and practice in the Neolithic Zagros. *Open Archaeol.* 11:20250041. doi: 10.1515/opar-2025-0041

Richardson, A., Matthews, R., Matthews, W., Walsh, S., Raeuf Aziz, K., and Stone, A. (2020). "Excavations and contextual analyses: Bestansur" in *The Early Neolithic of the Eastern Fertile Crescent: Excavations at Bestansur and Shimshara, Iraqi Kurdistan*, eds. R. Matthews, W. Matthews, K.R. Raheem and A. Richardson (Oxford: Oxbow Books) 115–176.

Rostami, H., Richter, T., Ruter, A. H., Azizi, G., Darabi, H., and Maleki, S. (2024). High-resolution, multi-proxy reconstruction of central Zagros paleoclimate and paleoenvironment from the Late Pleistocene to the Holocene. *Quat. Int.* 692, 45–55. doi: 10.1016/j.quaint.2024.02.003

Russell, W. A., Papanastassiou, D. A., and Tombrello, T. A. (1978). Ca isotope fractionation on the Earth and other solar system materials. *Geochim. Cosmochim. Acta* 42, 1075–1090. doi: 10.1016/0016-7037(78)90105-9

Saeed Ali, S. (2007). *Geology and hydrogeology of Sharazoor – Piramagroon Basin in Sulaimani area, Northeastern Iraq.* [PhD thesis]. Serbia: University of Belgrade.

Santana, J., Millard, A., Ibáñez-Estevez, J. J., Bocquentin, F., Nowell, G., Peterkin, J., et al. (2021). Multi-isotope evidence of population aggregation in the Natufian and scant migration during the Early Neolithic of the Southern Levant. *Sci. Rep.* 11:11857. doi: 10.1038/s41598-021-90795-2

Schoeninger, M. J., and Peebles, C. S. (1981). Effect of mollusc eating on human bone strontium levels. *J. Archaeol. Sci.* 8, 391–397. doi: 10.1016/0305-4403(81)90038-8

Schroeder, H. A., Tipton, I. H., and Nason, A. P. (1972). Trace metals in man: Strontium and barium. *J. Chronic Dis.* 25, 491–517. doi: 10.1016/0021-9681(72)90150-6

Sillen, A., and Kavanagh, M. (1982). Strontium and paleodietary research: A review. *Am. J. Phys. Anthropol.* 25, 67–90. doi: 10.1002/ajpa.1330250505

Sissakian, V. K., and Fouad, S. F. (2015). Geological map of Iraq, scale 1:1000 000, 2012. *Iraqi Bull. Geol. Min.* 11, 9–16

Sissakian, V. K., and Fouad, S. F. (2016). Geological map of Sulaimaniyah quadrangle, scale 1:250 000. *JZS-A* 1, 151–161. doi: 10.17656/jzs.10477

Spies, M. J., Alblas, A., Ambrose, S. H., Barakat, S., Barberena, R., Bataille, C., et al. (2025). Strontium isoscapes for provenance, mobility and migration: The way forward. *R. Soc. Open Sci.* 12:250283.

Tchernov, E. (1991). Of mice and men. Biological markers for long-term sedentism; a reply. *Paléorient* 17, 153–160. doi: 10.3406/paleo.1991.4548

Vaiglova, P., Kierdorf, H., Witzel, C., Falster, G., Joannes-Boyau, R., Wang, Y., et al. (2025). Transport of animals underpinned ritual feasting at the onset of the Neolithic in Southwestern Asia. *Commun. Earth Environ.* 6:519. doi: 10.1038/s43247-025-02501-z

Walsh, S. (2020). "Human remains from Bestansur: demography, diet and health," in *The Early Neolithic of the Eastern Fertile Crescent: Excavations at Bestansur and Shimshara, Iraqi Kurdistan*, eds. R. Matthews, W. Matthews, K.R. Raheem and A. Richardson (Oxford: Oxbow Books) 429–560.

Walsh, S. (2022). Early evidence of extra-masticatory dental wear in a Neolithic community at Bestansur, Iraqi Kurdistan. *Int. J. Osteoarchaeol.* 32, 1264–1274. doi: 10.1002/oa.3162

Walsh, S., and Matthews, R. (2018). "Articulating the disarticulated: Human remains from the Early Neolithic of the Eastern Fertile Crescent (Eastern Iraq and Western Iran)," in *Neolithic Bodies. Neolithic Studies Group Seminar Papers* 15, eds. P. Bickle and R. Sibbeson (Oxford: Oxbow Books) 60–73.

Wang, X., Skourtanioti, E., Benz, M., Gresky, J., Ilgner, J., Lucas, M., et al. (2023b). Isotopic and DNA analyses reveal multiscale PPNB mobility and migration across Southeastern Anatolia and the Southern Levant. *Proc. Natl. Acad. Sci. U.S.A.* 120: e2210611120. doi: 10.1073/pnas.2210611120

Wang, X., Zhang, B., Sun, Y., Ingman, T., Eisenmann, S., Lucas, M., et al. (2023a). Isotopic and proteomic evidence for communal stability at Pre-Pottery Neolithic Jericho in the Southern Levant. *Sci. Rep.* 13:16360. doi: 10.1038/s41598-023-43549-1

Wathen-Avila, C., Bengtsson, F., Isaksson, S., Vretemark, M., Eriksson, G., and Lidén, K. (2025). They came from near and far–Strontium isotope analysis of people buried at the early Christian site of Varnhem, southwestern Sweden. *J. Archaeol. Sci. Rep.* 67:105387. doi: 10.1016/j.jasrep.2025.105387

Watkins, T. (2023). Settling down in Southwest Asia: The Epipalaeolithic-Neolithic transformation. *Front. Hum. Dyn.* 5:1250167. doi: 10.3389/fhumd.2023.1250167

Whitlam, J., Diffey, C., Bogaard, A., and Charles, M. (2020). "The charred plant remains from Early Neolithic levels at Bestansur and Shimshara" in *The Early Neolithic of the Eastern Fertile Crescent: Excavations at Bestansur and Shimshara, Iraqi Kurdistan*, eds. R. Matthews, W. Matthews, K.R. Raheem and A. Richardson (Oxford: Oxbow Books) 411–428.

Wieser, M. E., Buhl, D., Bouman, C., and Schwieters, J. (2004). High precision calcium isotope ratio measurements using a magnetic sector multiple collector inductively coupled plasma mass spectrometer. *J. Anal. At. Spectrom.* 19, 844–851. doi: 10.1039/b403339f

Woodhead, J., Swearer, S., Hergt, J., and Maas, R. (2005). In situ Sr-isotope analysis of carbonates by LA-MC-ICP-MS: Interference corrections, high spatial resolution and an example from otolith studies. *J. Anal. At. Spectrom.* 20, 22–27. doi: 10.1039/b412730g

Yang, D., Podkovyroff, K., Uno, K. T., Bowen, G. J., Fernandez, D. P., and Cerling, T. E. (2025). Strontium isotope mapping of elephant enamel supports an integrated microsampling-modeling workflow to reconstruct herbivore migrations. *Commun. Biol.* 8:274. doi: 10.1038/s42003-025-07686-9

Zazzo, A., Le Corre, M., Lazzerini, N., Marchina, C., Bayarkhuu, N., Bernard, V., et al. (2025). 3000 yr-old patterns of mobile pastoralism revealed by multiple isotopes and radiocarbon dating of ancient horses from the Mongolian Altai. *PLoS ONE* 20:e0322431. doi: 10.1371/journal.pone.0322431

Zeder, M. A. (2024a). Out of the shadows: Reestablishing the Eastern Fertile Crescent as a center of agricultural origins: Part 2. *J. Archaeol. Res.* 33, pp. 159–247. doi: 10.1007/s10814-024-09198-2

Zeder, M. A. (2024b). Out of the shadows: Reestablishing the Eastern Fertile Crescent as a center of agricultural origins: Part 1. *J. Archaeol. Res.* 33, pp.1–56. doi: 10.1007/s10814-024-09195-5